Supporting information

NIR-I Light-Responsive Superoxide Radical Generator with Cancer Cell Membrane Targeting for Enhanced Imaging-Guided Photodynamic Therapy

Yingcui Bu[a], Tianren Xu[a], Xiaojiao Zhu*[a], Jie Zhang[b], Lianke Wang[b], Zhipeng Yu[b], Jianhua Yu[a], Aidong Wang[c], Yupeng Tian[a], Hongping Zhou*[a], and Yi Xie[d]

[a.] *College of Chemistry and Chemical Engineering, Institute of Physical Science and Information Technology, Anhui University and Key Laboratory of Functional Inorganic Materials Chemistry of Anhui Province, Anhui Province Key Laboratory of Chemistry for Inorganic/Organic Hybrid Functionalized Materials, Key Laboratory of Structure and Functional Regulation of Hybrid Materials (Anhui University) Ministry of Education, Hefei, 230601, P.R. China.*

[b.] *Institute of Physical Science and Information Technology, Anhui University, Hefei, 230601, P.R. China.*

[c.] *Huangshan University, Huangshan, 242700, P.R. China.*

[d.] *Hefei National Laboratory for Physical Sciences at Microscale, iChem, University of Science and Technology of China, Hefei, China*

1. General information

1.1 Materials

All general chemicals for organic synthesis and fluorescence detection including 2, 7-dichloro fluorescein diacetate (H_2DCF-DA), 9,10-anthracenediylbis (methylene) dimalonic acid (ABDA), dihydrorhodamine 123 (DHR123), superoxide dismutase (SOD), Vitamin C (Vc), Singlet Oxygen Sensor Green (SOSG), TraKine ™ Pro Live-cell Tubulin Staining kit (Green Fluorescence dye), Dihydroethidium (DHE), Hydroxyphenyl fluorescein (HPF), 5,5-Dimethyl-1-pyrroline N-oxide (DMPO), dulbecco's modified eagle medium (DMEM), Deoxyribonucleic acid (DNA) and 3-(4,5-dimethylthiazol-2-yl)-2,5-diphenyltetrazolium bromide (MTT), 2-(4-Amidinophenyl)-6-indolecar- bamidine dihydrochloride, (DAPI), Mito-Tracker Deep Red, Cell Mask™ Green Plasma Membrane Stain, Calcein - AM/PI Double Stain Kit and apoptosis/necrosis kit (Annexin V-FITC/PI) were obtained from commercial sources (Aladdin, Macklin, Sigma-Aldrich, Bioquest and Thermo). Human cervical cancer cell (HeLa cells) and human hepatocellular carcinoma cell (Hep G2) were purchased from BeNa culture collection; human basal cell carcinoma (A431) were obtained from JeDbio corporation; human emborynic kidney (HEK 293T), mouse embryonic fibroblast (3T3), human embryonic lung fibroblast (HFL-1) and Human embryonic lung fibroblast (Helf) were purchased from the American type culture collection; and BALA/c nude mice were given by Shanghai sipul-bikai laboratory animal *Co., Ltd*. All the other solvents and reagents in this study are of analytical grade and used without further purification.

1.2 Instrumentation

The nuclear magnetic resonance (NMR) spectra were measured on a Bruker AVANCE instruments using the dimethyl sulfoxide-d_6 (DMSO-d_6) as solvents (400 MHz for ^{1}H NMR and 100 MHz for ^{13}C NMR). Mass spectra were performed on a mass spectrometer with LTQ Orbitrap XL. One-photon (OP) absorption (OPA) spectra were measured using UV-265 spectrophotometer. One-photonexcited fluorescence (OPEF) spectra were recorded on a Hitachi F-4500 fluorescence spectrophotometer. Two-photon (TP) emission fluorescence (TPEF) spectra were analyzed with femtosecond laser pulse and Ti: sapphire system (680-1080 nm, 80 MHz, 140 fs) as the light source. The molecular docking simulation was performed on a Biovia *Co* software (version 2016). EPR spectrum was recorded on a Bruker Nano x-band spectrometer. Confocal fluorescence imaging was showed on ZEISS710 and Olympus FV 1200 MPE-share confocal laser scanning microscope (CLSM).

2. Experimental and methods

2.1 Two-photon Action Cross-section

Two-photon (TP) action cross-sections of **EBD-1** and **EBD-5** were acquired through the two-photon excited fluorescence (TPEF) method with femtosecond laser piles and a Ti: sapphire system (680-1080 nm, 80 MHz, 140 fs) as the light source. Two-photon action cross-section (σ) value was calculated *via* the following equation [S1]:

$$\sigma\Phi = \sigma_{ref}\,\Phi_{ref}\,\frac{c_{ref}\,n_{ref}\,F}{c\,n\,F_{ref}} \qquad (1)$$

Where Φ is fluorescence quantum yield, c is the concentration of the solution (mol·L^{-1}), n is the refractive index, F is the integrated area under the corrected emission spectrum, the subscripts *ref* stands for the reference molecule (Rhodamine B). The fluorescence spectra of the reference and dyes that induced by two-photon were emitted at the same excitation wavelength.

2.2 DFT Calculation.

The ground state structures of **EBD-1~EBD-5** were optimized using DFT with B3LYP functional and 6-31G basis set. The initial geometries of the compounds were generated by the Gauss View software. The excited state related calculations (UV-vis absorption) were carried out with the time dependent DFT (TD-DFT) with the optimized structure of the ground state (DFT/6-31G). The emission of the fluorophore was calculated based on the optimized S1 excited state geometry. All the calculations were carried out in virtue of Gaussian 09.

2.3 *N*-octanol-Water Partition Coefficients of Dyes

Solid sample (2 mg) was added into a 10 mL centrifuge tube containing *n*-octanol (5 mL). The samples were placed

in a shaking table and shaken for 24 hours. After finished, the mixture solution, including 3mL of supernatant and 3mL distilled water, was centrifuged repeatedly for 5-6 times. Lastly, the absorbance of two layers were measured ($Abs_{\ n\text{-octanol}}$ /$Abs_{\ water}$), respectively, and the *log P* values were calculated following the formula:

$$lg\ P = lg\ \frac{Abs_{\ n\text{-octano}}}{Abs_{\ water}} \qquad (2)$$

2.4 Molecular Docking Simulation with DNA

The structure of DNA (ID: 1BNA, d (CGCGAATTCGCG) were retrieved from PDB database [S2]. All water molecules were then deleted. The structure of DNA was processed. The active-site cavities of DNA are defined using the biggest cavity of the surface of DNA. To demonstrate the specific recognition of ligand **EBD-1** or **EBD-5** with DNA (1BNA), respectively, docking was carried out using the method of CDOCK *via* software (version 2016, The Biovia Co.). The parameter was set as default. At the meanwhile, the binding energy is calculated between ligand with DNA. Binding energy is actually the energy of the entire complex minus the energy of the individual ligands and the individual proteins: Binding Energy = complex energy- (ligand energy + protein energy). Firstly, ten optimal binding conformations were selected to obtain the binding energies of the ten conformations according to the software's built-in program (calculation binding energy). Then, the average binding energy of the 10 optimal configurations are calculated to get the average binding energy.

2.5 Fluorescence titration of PSs with DNA

Stock solution of **EBD-1** and **EBD-5** (1×10^{-3} M) were prepared in DMSO. A series of test solutions were prepared by dissolving 50 μL stock solutions of two PSs in 5.00 mL distilled water. Then DNA (10^{-2} M) with different volume was added in the 5.00 mL test solution. Lastly, the fluorescence intensity was recorded on a Hitachi F-4500 fluorescence spectrophotometer. The sequence of DNA (calf thymus) is provided in the following. (CAS: 73049-39-5)

1 aattcaggat gcctcttgtg ttggcctagg caagtccaat cttccactcg agttgcgaag

61 gaaagctggg cattgctctc gagtgactgc agggccaata gacgtcatct aggcttgtgt

121 ccagaagcca atgttcctct ccaggggcga cagggatctc ggggttgcat tccagacgca

181 cccggggaga caggcattca tctcgagtgg aagcaaagaa ccccgctctg ctctcgaatc

241 gcgacgggta tctcttggag ctcactgggt ggactcaagg gagtcaagcc tcctgaggcg

301 tttggagaga ggccgcgaga ttggtctcta ggccatgcag gagacgaagg ccctcactct

361 cgataacggc ggaatctcgg ggttgttctc gagcggcggc cccagtgtgc ggtttctcac

421 gaggtacgac ggcgaggtca gtgagcctct cgtggggcgc cagggaagtc gggtctccat

481 gcgagtggcg agggggagcg cgtcattgct cgcgagccat gggaggggac tctggcctcg

541 agacgtgttg aagaaggtct ctcgaggtct ttcccgggtt gaggcaggaa accctgggtt

601 ccctcgactt gtgcaggtga cctcagggga cttctcatgg tggctctgcg aagccaggga

661 aactggaggt gggaggggcc tctcgggact ccactgggtt tggtgcattg gaagagggcc

2.6 *In vitro* $^1O_2$ Detection and Quantum Yield Evaluation

The $^1O_2$ detection experiment was performed taking advantage of commercial $^1O_2$ indicator ABDA. Firstly, 3 mL dyes (10 μM) were added into 5 mL centrifuge tubes and 13 μL of ABDA stock solution (7.5 mM) was added in dark condition. Then the cuvette was exposed to white light irradiation for different time (10, 20, 30, 40, 50, 60 s) and standard photosensitizer Rose Bengal (RB) was employed as control. The absorption spectra of ABDA at 378 nm with different irradiation time were obtained and subsequently the decay rates of photosensitizers were calculated. The $^1O_2$ quantum yield of **EBD-1**~**EBD-5** in water was evaluated according to the following formula:

$$\Phi_{PS} = \Phi_{RB} \frac{K(PS)\, A(RB)}{K(RB)\, A(PS)} \quad (3)$$

Where *K(PS)* and *K(RB)* are the decay rate constants of ABDA by the targeted molecules **EBD-1**~**EBD-5** and RB. *A(PS)* and *A(RB)* represent the integral area of the absorption bands in the wavelength range of 400 - 700 nm. Φ_{RB} is the $^1O_2$ quantum yield of RB (75%) in H_2O.

2.7 *In vitro* $O_2^{-\bullet}$ Detection using DHR 123

The $O_2^{-\bullet}$ detection experiment was performed using commercial $O_2^{-\bullet}$ indicator DHR123 which could be transformed to rhodamine 123 in the presence of $O_2^{-\bullet}$. During experimental process, **EBD-1**~**EBD-5** (10 μM) and DHR123 (5×10^{-5} M) were prepared in distilled water. Then the cuvette was exposed to irradiation for different time (10, 20, 30, 40, 50, 60, 70 s), and the fluorescence spectra were recorded right away. For $O_2^{-\bullet}$ quenching experiment, 10 μM of SOD and 50 μM Vc were added ahead of irradiation.

2.8 Detecting $O_2^{-\bullet}$ Generation via Electron Paramagnetic Resonance (EPR) Assay

The EPR assay was carried out with a Bruker Nano x-band spectrometer using 5,5-dimethyl-1-pyrroline N-oxide (DMPO) as a spin-trap agent. **EBD-1** was dissolved in methanol at a dilution of 10^{-5} M, and then 25 mM DMPO was added into methanol without and with irradiation (808 nm laser; 200 mW/cm^2) for 60 s. Finally, the EPR signal was recorded at room temperature.

2.9 Dark Cytotoxicity Evaluation

The cytotoxicity effects of **EBD-1**~**EBD-5** were evaluated by HeLa cells, A431, Hep G2, HEK 293T, 3T3, HFL-1 and Helf using a MTT assay. All cell lines were planted in the 96-well plate with a density of 10^4 cells per well and incubated for another 12 h at 37 °C, 5% CO_2. Then, **EBD-1**~**EBD-5** with various concentrations (0, 5, 10, 15, 20, 25 μM) were added and grown for 24 h. MTT with 10 μL (5 mg/mL in PBS) was added for an additional 4 h. Subsequently, 150 μL of DMSO was added to dissolve the purple formazan crystals. Finally, the absorption of each well was recorded at 490 nm on a multidetection microplate reader (Bio-Rad 550).

2.10 Light Cytotoxicity Evaluation

HeLa cells were seed in the 96-well plate at a density of 10^4 cells per well. After 12 h of incubation, PSs with 0, 10 μL were added in various wells and incubated for another 30 min at 37 °C, 5% CO_2. Then plates including HeLa cells were exposed to light irradiation (808 nm laser; 200 mW/cm^2) for 20 min and 40 min, respectively and in dark for control. Lastly, the same treatments were carried out.

2.11 Intracellular ROS Detection

H_2DCF-DA was applied for the intracellular ROS detection. HeLa cells were seeded in the glass bottom dishes and incubated about 48 h for adhering. Then HeLa cells were incubated with 10 μM **EBD-1** and **EBD-5** for 30 min for cell uptake followed by incubation with 10 μM H_2DCF-DA for 30 min. After that, cells were washed with PBS and then irradiated for 30 min. For free radical scavenging experiment, 50 μM Vc were added to above similar cell culture dish ahead of light irradiation. The green fluorescence was immediately observed using CLSM. (λ_{ex} = 504 nm; λ_{ex} = 529 nm).

2.12 Intracellular $^1O_2$ Imaging

SOSG was employed as the intracellular $^1O_2$ indicator. HeLa cells were seeded in the glass bottom dishes and incubated about 48 h for adhering. Then HeLa cells were incubated with 10 μM **EBD-1** and **EBD-5** for 30 min for cell uptake followed by incubation with 2 μM SOSG for 30 min. After that, cells were washed with PBS and then irradiated with 808 nm irradiation for 30 min. For $^1O_2$ scavenging experiment, 50 μM NaN_3 was added to above similar cell culture dish at 37 °C for 2 h ahead of irradiation. The green fluorescence was immediately observed using CLSM. (λ_{ex} = 504 nm; λ_{ex} = 525 nm).

2.13 Intracellular $O_2^{-\bullet}$ detecting

HeLa cells were pretreated with **EBD-1** (10 μM) for 30 min and then co-stained with DHE (10 μM) for another 30

min. Afterwards, HeLa cells were irradiated with 808 nm laser (200 mW/cm^2) for different time, which were then imaged under CLSM. (λ_{ex} = 488 nm, λ_{em} = 570-620 nm)

2.14 Intracellular OH˙ detecting

HeLa cells were pretreated with **EBD-1** (10 μM) for 30 min and then co-stained with HPF (10 μM) for another 60 min. After that, HeLa cells were irradiated with 808 nm laser (200 mW/cm^2) for different time, which were then imaged under CLSM. (λ_{ex} = 488 nm, λ_{em} = 650-700 nm)

2.15 Cell Culturing and Imaging

Seven cells lines were cultured in cell culture dishes with Dulbecco's modified eagle medium (DMEM) medium containing 10 % fetal bovine serum (FBS) and incubated at 37 °C in air atmosphere (5% CO_2). In fluorescence imaging experiments, the cells were planted into glass bottom dishes (15 × 15 mm) at density of 10^4 for confocal and co-location experiments and at density of 10^6 for live/dead experiment (AM/PI). After 10 μM of **EBD-1** and **EBD-5** were added and cultivated for 30 min at 37 °C, the dishes were washed with PBS (pH 7.2) for three times. The cell images were acquired via ZEISS710 and Olympus FV 1200 MPE-share confocal laser scanning microscope with 10× or 60 × objective lens.

2.16 Subcellular Colocalization Assay

HeLa cells were seeded into 15mm × 15mm confocal dishes and incubated for 48 h. After incubated with 10 μM PSs for 30 min in a 5% CO_2 atmosphere at 37 °C, the cells were further stained by 1μM DAPI (λ_{ex} = 340 nm; λ_{ex} = 488 nm), 1μM Mito-Tracker Deep Red dye (λ_{ex} = 640 nm; λ_{ex} = 659 nm), 1μM Cell Mask ™ Green (λ_{ex} = 522 nm; λ_{ex} = 535 nm). Finally, HeLa cells were visualized with laser confocal microscopy.

2.17 ROS Induced Cytoskeleton Collapse Experiment

HeLa cells were seeded in 15 mm×15 mm glass bottom dishes to incubation 24 h. Then **EBD-1** was added to co-culture for 30 min, after that, the culture media was discard and washed with PBS and media (-) (Cell culture media without FBS) for one time. Staining solution was added into the glass bottom dishes incubated in a 37 ℃, 5 % CO_2 atmosphere for 1 h. Next, removed the staining solution and washed with media (-) once, incubated the cells with media (-) for another 15 min. Subsequently, removed the media (-) and washed with media (+) (Cell culture media with 10% FBS) once, incubating with media (+) for 45 min. Finally, HeLa cells were imaged by microscope.

2.18 Live/Dead cell Co-staining for Evaluating Photon-induced Cell Death

For live/dead cells co-staining assay, using Calcein-AM for live cells, one of the Calcein-AM/PI Double Stain Kit

and **EBD-1** for dead cells, which could play the role of PI and exhibited red fluorescence in nucleus during cell apoptosis. Briefly, HeLa cells were planted onto confocal dishes and incubated for 48 h. Then the cells were further treated with 400 uL dye diluent and 10 uL Calcein-AM stain after 10 uL **EBD-1** was added for 30 min. Co-incubated for 20 min, the cell image was observed immediately using CLSM. (Calcein-AM: λ_{ex} = 490 nm; λ_{ex} = 520 nm, **EBD-1**: λ_{ex} = 488 nm; λ_{ex} = 630 nm)

2.19 Mechanisms of Cell Death using Apoptosis/Necrosis Kit (Annexin V-FITC/PI)

HeLa cells were planted onto confocal dishes and grew to suitable density (1×10^4 cells). Then **EBD-1** (10 μM) was added to co-culture for 30 min, which was subsequently disposed with 400 μL binding buffer and stained by 10 μL Annexin V-FITC (λ_{ex} = 488 nm, λ_{em} = 530 nm) and 5 μL PI (λ_{ex} = 488 nm, λ_{em} = 650-700 nm) in a cool and dark atmosphere for 15 min. Lastly, the co-stained HeLa cells were observed by CLSM and traced with different irradiation time.

2.20 Animals and Tumor Model

~~All animals (BALB/c mice of 4-5 week old) were obtained from Shanghai sipul-bikai laboratory animal Co., Ltd. Animal studies were performed in compliance with the relevant laws and institutional guidelines set by Anhui Committee of Use and Care of Laboratory Animals and the overall project protocols were approved by the College of Life Science, Anhui University.~~ The A431 tumor-bearing mice were obtained by subcutaneously injecting A431 cells (1×10^6 cells) in subcutaneous injections of female mice.

2.21 *In vivo* Fluorescence Imaging

Mice with A431 transplanted tumor were subcutaneously injected with **EBD-1**-based PS, PBS, and then were anesthetized with 2.5% isofluorane in oxygen at selected time points. Subsequently, the whole-body fluorescence images were captured using an LB983 NC100 imaging system (Berthold co. Ltd.). After the 24 h later, mice were sacrificed and their hearts, livers, spleens, lungs, kidneys and tumors were collected. Ex vivo fluorescence imaging of these organs was immediately performed on the LB983 NC100 imaging system.

2.22 Antitumor Therapy

Cells suspension (10^8 cells/mL, A431 cells) was obtained and then subcutaneously injected at the female BALB/c nude mice (4-5-week old). Then the A431-bearing mice were kept in SPF condition, protected from light and fed and watered freely. After 5-days inoculation, the tumor size was appropriate and the tumor nude mice were split into four groups (3 mice each), treated as below: (a) Control, (b) **EBD-1** (10^{-3} M, 100 μL), (c) 808 nm fs laser (d) **EBD-1**+808 nm fs laser. It's worth noting that only a single-dose injection was employed during *in vivo* treatment process.

The changes of tumor volume, tumor weight and body weight were measured every 5 days during treatment. After treatment, major organs and tumors were gathered for H&E staining.

2.23 Hematoxylin and eosin (H&E) staining.

After 20 days PDT treatment, the mice in different groups were sacrificed and the tissues were collected and fixed in 4 % paraformaldehyde. Subsequently, the obtained tissues were embedded into paraffin, sliced at a thickness of 5 μm, which were stained with hematoxylin and eosin (H&E).

3 Synthesis

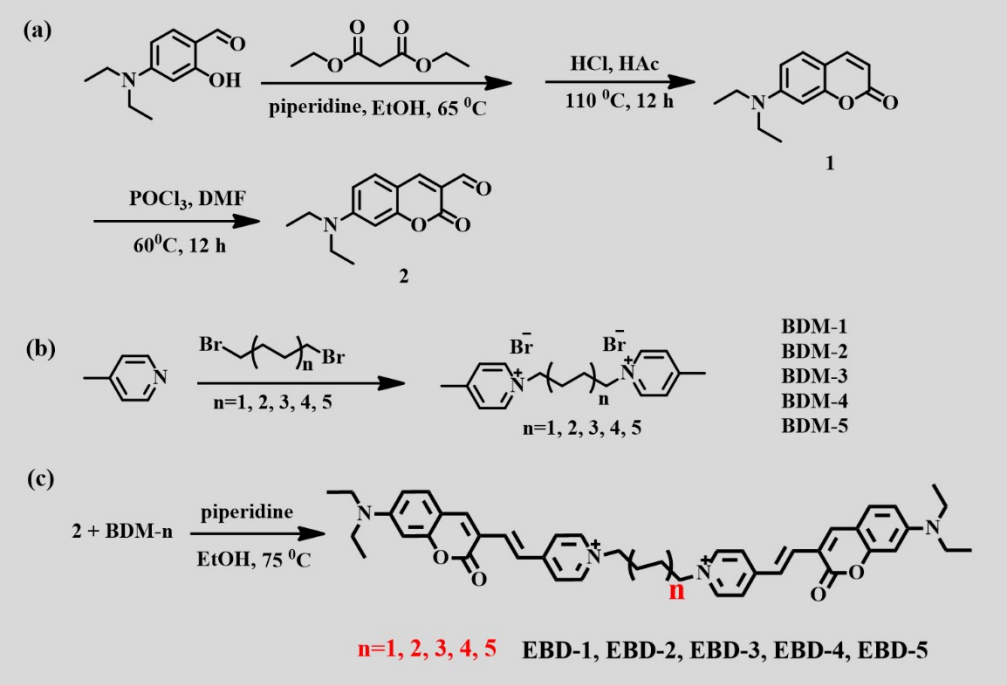

Scheme S1 The synthetic routes for compounds **EBD-1**~**EBD-5**.

3.1 Synthesis of BDM-1

1, 4-dibromo-butane (2.0 g, 9.26 mmol) and 4-methyl-pyridine (1.98 g, 21.30 mmol) were dissolved in ethanol (1.0 mL) and refluxed at 80 ℃ for 2 h. After quench of the reaction, the reaction solution was washed three times with ethyl acetate and afforded a white solid (3.41 g, yield = 91.5 %). ^{1}H NMR (400 MHz, DMSO-d_6), δ (ppm) (**Fig. S1**): 8.96-8.94 (d, J = 8.00 Hz, 4H), 8.02-8.00 (d, J = 8.00 Hz, 4H), 4.60 (s, 4H), 2.61 (s, 6H), 1.91 (s, 4H); ^{13}C NMR (100 MHz, DMSO-d_6), δ (ppm) (**Fig. S2**): 158.90, 143.75, 128.38, 58.99, 27.00, 21.30; MS (ESI) (**Fig. S3**): calcd for: $C_{16}H_{22}N_2^{2+}$ [M/2], 121.09; found, 121.0882.

3.2 Synthesis of BDM-2

1, 6-dibromo-hexane (2.0 g, 8.20 mmol) and 4-methyl-pyridine (1.76 g, 18.85 mmol) were dissolved in ethanol (1.0 mL) and refluxed at 80 ℃ for 2 h. After quench of the reaction, the reaction solution was washed three times with

ethyl acetate and afforded a white solid (3.35 g, yield = 94.9 %). ^{1}H NMR (400 MHz, DMSO-d_6), δ (ppm) (**Fig. S4**): 8.90-8.88 (d, J = 8.00 Hz, 4H), 7.95-7.94 (d, J = 4.00 Hz, 4H), 4.83 (s, 4H), 4.63-4.60 (t, J = 6.00 Hz, 4H), 2.05-2.01 (t, J = 16.00 Hz, 4H), 1.50-1.46 (t, J = 16.00 Hz, 4H); ^{13}C NMR (100 MHz, DMSO), δ (ppm) (**Fig. S5**): 159.79, 143.50, 128.50, 60.43, 30.52, 24.93, 20.59; MS (ESI) (**Fig. S6**): calcd for: $C_{18}H_{26}N_2^{2+}$ [M/2], 135.1; found, 135.1040.

3.3 Synthesis of BDM-3

1, 8-dibromo-octane (2.0 g, 7.35 mmol) and 4-methyl-pyridine (1.57 g, 16.91 mmol) were dissolved in ethanol (1.0 mL) and refluxed at 80 ℃ for 2 hr. After quench of the reaction, the reaction solution was washed three times with ethyl acetate and afforded a white solid (3.0 g, yield = 90.1 %). ^{1}H NMR (400 MHz, DMSO-d_6), δ (ppm) (**Fig. S7**): 8.99-8.97 (d, J = 8.00 Hz, 4H), 8.01-7.99 (d, J = 8.00 Hz, 4H), 4.56-4.52 (t, J = 8.00 Hz, 4H), 2.61 (s, 6H), 1.89-1.86 (t, J = 6.00 Hz, 4H), 1.27 (s, 8H); ^{13}C NMR (100 MHz, DMSO-d_6), δ (ppm) (**Fig. S8**): 158.90, 143.59, 128.32, 59.95, 30.33, 27.94, 24.87, 21.11; MS (ESI) (**Fig. S9**): calcd for: $C_{20}H_{30}N_2^{2+}$ [M/2], 149.1; found, 149.1195.

3.4 Synthesis of BDM-4

1, 10-dibromo-decane (2.0 g, 6.67 mmol) and 4-methyl-pyridine (1.43 g, 15.33 mmol) were dissolved in ethanol (1.0 mL) and refluxed at 80 ° C for 2 h. After quench of the reaction, the reaction solution was washed three times with ethyl acetate and afforded a white solid (2.89 g, yield = 89.0 %). ^{1}H NMR (400 MHz, DMSO-d_6), δ (ppm) (**Fig. S10**): 8.95-8.93 (d, J = 8.00 Hz, 4H), 7.96-7.95 (d, J = 4.00 Hz, 4H), 4.52-4.49 (t, J = 6.00 Hz, 4H), 2.46 (s, 6H), 1.87-1.80 (t, J = 14.00 Hz, 4H), 1.21-1.19 (d, J = 8.00 Hz, 12H); ^{13}C NMR (100 MHz, DMSO-d_6), δ (ppm) (**Fig. S11**): 159.26, 144.22, 128.85, 60.37, 31.14, 29.23, 28.90, 25.92, 21.92; MS (ESI) (**Fig. S12**): calcd for: $C_{20}H_{34}N_2^{2+}$ [M/2], 163.2589; found, 163.1363.

3.5 Synthesis of BDM-5

1, 12-dibromo-dodecane (2.0 g, 6.10 mmol) and 4-methyl-pyridine (1.30 g, 14.02 mmol) were dissolved in ethanol (1.0 mL) and refluxed at 80 ℃ for 2 hr. After quench of the reaction, the reaction solution was washed three times with ethyl acetate and afforded a white solid (2.68 g, yield = 85.5 %). ^{1}H NMR (400MHz, DMSO-d_6), δ (ppm) (**Fig. S13**): 8.96-8.94 (d, J = 8 Hz, 4H), 8.00-7.99 (d, J = 4 Hz, 4H), 4.55-4.51 (t, J = 8 Hz, 4H), 2.61 (s, 6H), 1.89-1.86 (t, J = 6 Hz, 4H), 1.25-1.22 (d, J = 12 Hz, 16H); ^{13}C NMR (100 MHz, DMSO-d_6), δ (ppm) (**Fig. S14**): 158.74, 143.66, 128.31, 59.86, 30.54, 28.87, 28.78, 28.38, 25.37, 21.33; MS (ESI) (**Fig. S15**): calcd for: $C_{24}H_{38}N_2^{2+}$ [M/2], 177.15; found, 177.1508.

3.6 Synthesis of EBD-1

BDM-1 (1.0 g, 2.5 mmol) and compound 2 (1.3 g, 5.3 mmol) were dissolved in ethanol (15 mL) and then six drops of piperidine was added into the system. The mixture was stirred at 75 ° C for 4 h. After accomplished, the resulting

mixture was filtered and the obtained crude was purified by recrystallization with ethanol (60 mL) and methanol (10 mL) to afford the red solid **EBD-1** (2.0 g, 93.0 %). ^{1}H NMR (400 MHz, DMSO-d_6), δ (ppm) (**Fig. S16**): 8.90-8.89 (d, J = 6.48 MHz, 4 H), 8.24-8.18 (t, J = 11.22 MHz, 6 H), 7.88-7.84 (d, J = 16.00 MHz, 2 H), 7.72-7.68 (d, J = 16.00 MHz, 2 H), 7.56-7.54 (d, J = 13.32 MHz, 2 H), 6.82-6.79 (m, J = 13.32 MHz, 2 H), 6.61 (s, 2 H), 4.54 (s, 4 H), 3.52-3.47 (m, J = 13.32 MHz, 8 H), 1.95 (s, 4 H), 1.17-1.14 (t, J = 13.32 MHz, 12 H). ^{13}C NMR (100 MHz, DMSO-d_6), δ (ppm)(**Fig. S17**): 159.57, 156.32, 153.44, 152.01, 145.46, 144.00, 137.09, 130.75, 123.34, 122.57, 113.62, 110.05, 108.35, 96.22, 58.60, 44.35, 26.98, 12.35. MS (ESI) (**Fig. S18**): calcd for: $C_{44}H_{48}N_4O_4^{2+}$ [M/2], 348.1833; found, 348.1856.

3.7 Synthesis of EBD-2

BDM-2 (1.0 g, 2.3 mmol) and compound 2 (1.3 g, 5.3 mmol) were dissolved in ethanol (15 mL) and then six drops of piperidine was added into the system. The mixture was stirred at 75 ^{o} C for 4 h. Tracked by thin-layer chromatography (TLC), when finished, the mixture was filtered to get the crude product. After recrystallization with ethanol (60 mL) and methanol (10 mL), **EBD-2** was obtained as a red powder (1.79 g, 88.0 %). ^{1}H NMR (400 MHz, DMSO-d_6), δ (ppm) (**Fig. S19**): 8.90-8.88 (d, J = 6.48 MHz, 4 H), 8.23-8.17 (t, J = 11.22 MHz, 6 H), 7.87-7.83 (d, J = 16.00 MHz, 2 H), 7.71-7.67 (d, J = 16.00 MHz, 2 H), 7.56-7.53 (d, J = 13.32 MHz, 2 H), 6.82-6.79 (m, J = 13.32 MHz, 2 H), 6.60 (s, 2 H), 4.49-4.45 (t, J = 13.32 MHz, 4 H), 3.52-3.47 (m, J = 13.32 MHz, 8 H), 1.90 (s, 4 H), 1.32 (s, 4 H), 1.17-1.13 (t, J = 13.32 MHz, 12 H). ^{13}C NMR (100 MHz, DMSO-d_6), δ (ppm)(**Fig. S20**): 159.57, 156.31, 153.36, 152.00, 145.41, 143.93, 137.02, 130.73, 123.27, 122.58, 113.64, 110.03, 108.35, 96.22, 59.30, 44.35, 30.08, 24.90, 12.35. MS (ESI) (**Fig. S21**): calcd for: $C_{46}H_{52}N_4O_4^{2+}$ [M/2], 362.1990; found, 362.2015.

3.8 Synthesis of EBD-3

BDM-3 (1.0 g, 2.2 mmol) and compound 2 (1.3 g, 5.3 mmol) were dissolved in methanol (15 mL) and then six drops of piperidine was added into the system. The mixture was stirred at 75 ^{o}C for 4 h. After accomplished, the resulting mixture was filtered and the obtained crude was purified by recrystallization with ethanol (60 mL) and methanol (10 mL) to afford the red solid **EBD-3** (1.87 g, 85.1 %). ^{1}H NMR (400 MHz, DMSO-d_6), δ (ppm) (**Fig. S22**): 8.92-8.90 (d, J = 6.48 MHz, 3 H), 8.25-8.18 (t, J = 11.22 MHz, 6 H), 7.89-7.84 (d, J = 16.00 MHz, 2 H), 7.71-7.67 (d, J = 16.00 MHz, 2 H), 7.56-7.54 (d, J = 13.32 MHz, 2 H), 6.82-6.79 (m, J = 13.32 MHz, 2 H), 6.61-6.60(d, J = 16.00 MHz, 2 H), 4.49-4.46 (t, J = 16.00 MHz, 4 H), 3.52-3.47 (m, J = 13.32 MHz, 8 H), 1.91-1.88 (m, J = 16.00 MHz, 4 H), 1.30 (s, 8 H), 1.17-1.14(t, J = 16.00 MHz, 12 H). ^{13}C NMR (100 MHz, DMSO-d_6), δ (ppm)(**Fig. S23**): 159.57, 156.31, 153.32, 151.98, 143.92, 136.98, 130.74, 123.30, 122.58, 113.64, 110.04, 108.36, 96.22, 59.37, 44.35, 30.41, 28.14, 25.31, 12.35. MS (ESI)(**Fig. S24**): calcd for: $C_{48}H_{56}N_4O_4^{2+}$ [M/2], 376.2146; found, 376.2156.

3.9 Synthesis of EBD-4

BDM-4 (1.0 g, 2.1 mmol) and compound **2** (1.2 g, 5.2 mmol) were dissolved in methanol (15 mL) and then six drops of piperidine was added into the system. The mixture was stirred at 75 ^{o} C for 4 h. Tracked by thin-layer chromatography (TLC), when accomplished, the mixture was filtered to get the crude product which was further purified by recrystallization with ethanol (60 mL) and methanol (10 mL) to afford the red solid **EBD-4** (1.64 g, 83.2 %). ^{1}H NMR (400 MHz, DMSO-d_6), δ (ppm) (**Fig. S25**): 8.91-8.89 (d, J = 6.48 MHz, 4 H), 8.24-8.18 (t, J = 11.22 MHz, 6 H), 7.88-7.84 (d, J = 16.00 MHz, 2 H), 7.71-7.67 (d, J = 16.00 MHz, 2 H), 7.56-7.54 (d, J = 13.32 MHz, 2 H), 6.82-6.79 (m, J = 13.32 MHz, 2 H), 6.61-6.60 (d, J = 16.00 MHz, 2 H), 4.49-4.45 (t, J = 16.00 MHz, 4 H), 3.52-3.47 (m, J = 13.32 MHz, 8 H), 1.91-1.88 (t, J = 16.00 MHz, 4 H), 1.27-1.26 (d, J = 13.32 MHz, 12 H), 1.17-1.13 (t, J = 16.00 MHz, 12 H). ^{13}C NMR (100 MHz, DMSO-d_6), δ (ppm)(**Fig. S26**): 159.57, 156.31, 153.31, 151.98, 143.92, 136.97, 130.74, 122.59, 113.64, 110.04, 108.35, 96.23, 59.42, 44.35, 30.47, 28.63, 28.31, 25.40, 12.35. MS (ESI) (**Fig. S27**): calcd for: $C_{50}H_{60}N_4O_4^{2+}$ [M/2], 390.2302; found, 390.2340.

3.10 Synthesis of EBD-5

BDM-5 (1.02 g, 1.91 mmol) and compound 2 (1.10 g, 5.13 mmol) were dissolved in methanol (15 mL) and then six drops of piperidine was added into the system. The mixture was stirred at 75 ^{o} C for 4 h. when accomplished, the mixture was filtered to obtain the crude product which was further purified by recrystallization with ethanol (60 mL) and methanol (10 mL) to afford the red solid **EBD-5** (1.44 g, 78.4 %). ^{1}H NMR (400 MHz, DMSO-d_6), δ (ppm) (**Fig. S28**): 8.90-8.89 (d, J = 6.48 MHz, 4 H), 8.25-8.18 (t, J = 11.22 MHz, 6 H), 7.88-7.84 (d, J = 16.00 MHz, 2 H), 7.71-7.67 (d, J = 16.00 MHz, 2 H), 7.56-7.54 (d, J = 13.32 MHz, 2 H), 6.82-6.79 (m, J = 13.32 MHz, 2 H), 6.61-6.60 (d, J = 16.00 MHz, 2 H), 4.49-4.45 (t, J = 16.00 MHz, 4 H), 3.52-3.47 (m, J = 13.32 MHz, 8 H), 1.90-1.87 (t, J = 16.00 MHz, 4 H), 1.27-1.24 (d, J = 13.32 MHz, 16 H), 1.17-1.13 (t, J = 16.00 MHz, 12 H).^{13}C NMR (100 MHz, DMSO-d_6), δ (ppm) (**Fig. S29**): 159.57, 156.31, 153.30, 151.98, 145.41, 143.91, 136.96, 130.74, 123.29, 122.60, 113.64, 110.04, 108.35, 96.23, 59.43, 44.35, 30.47, 28.83, 28.76, 28.37, 25.41, 12.35. MS (ESI) (**Fig. S30**): calcd for: $C_{52}H_{64}N_4O_4^{2+}$ [M/2], 404.2461; found, 404.2471.

The compound **2** was synthesize according to previous study [S3].

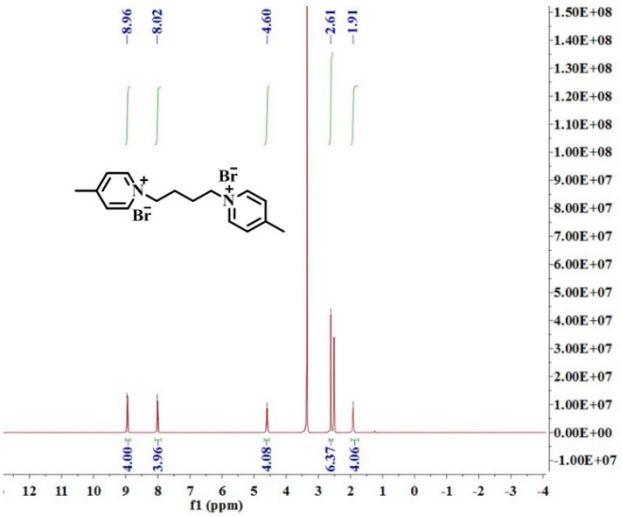

Figure S1 The 400 MHz ^{1}H NMR spectrum of **BDM-1** in the DMSO-d_6 solution.

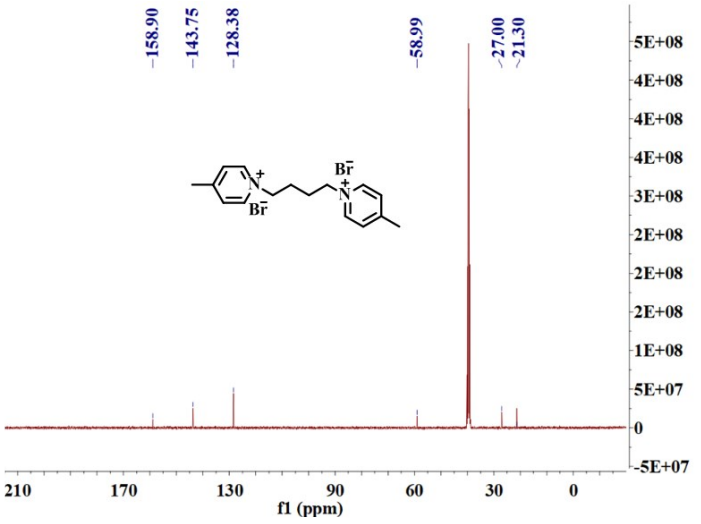

Figure S2 The 100 MHz ^{13}C NMR spectrum of **BDM-1** in the DMSO-d_6 solution.

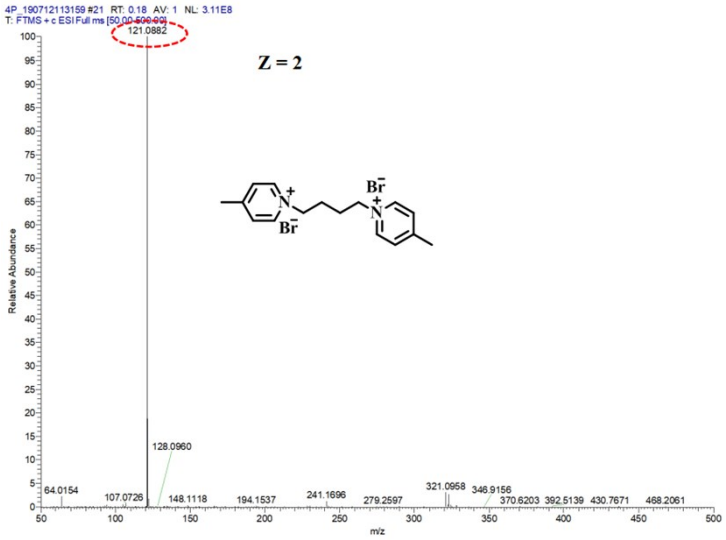

Figure S3 ESI-Mass spectrum of **BDM-1**.

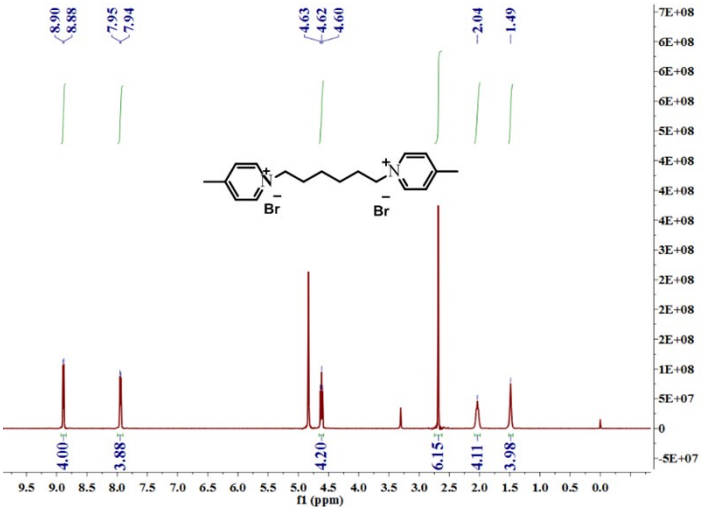

Figure S4 The 400 MHz ^{1}H NMR spectrum of **BDM-2** in the DMSO-d_6 solution.

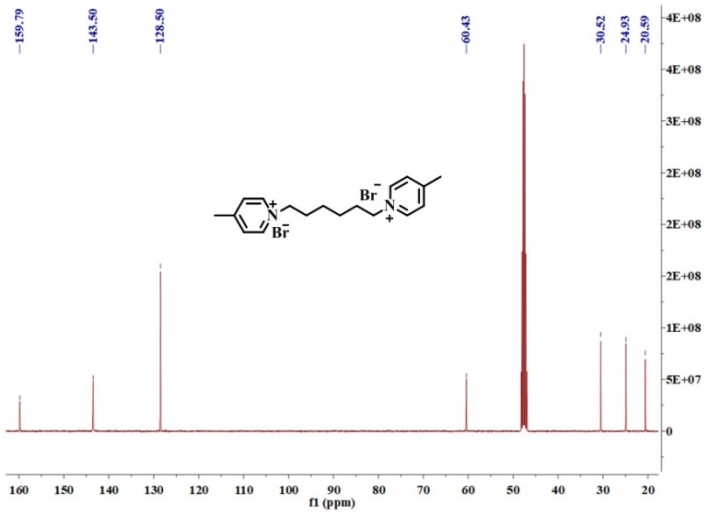

Figure S5 The 100 MHz ^{13}C NMR spectrum of **BDM-2** in the DMSO-d_6 solution.

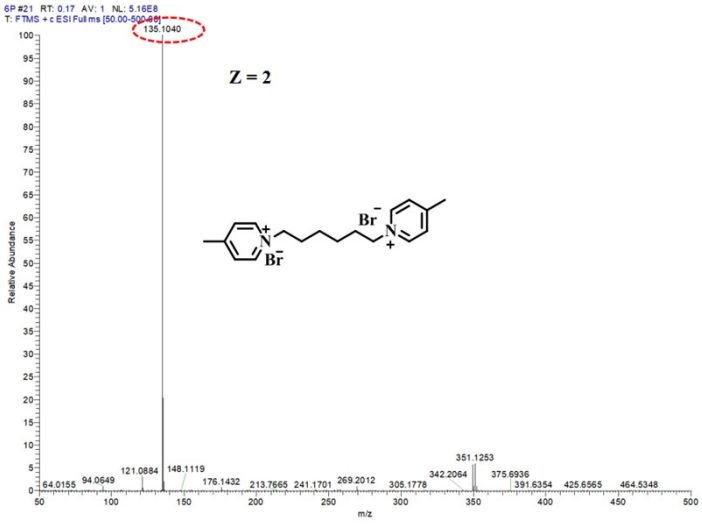

Figure S6 ESI-Mass spectrum of **BDM-2**.

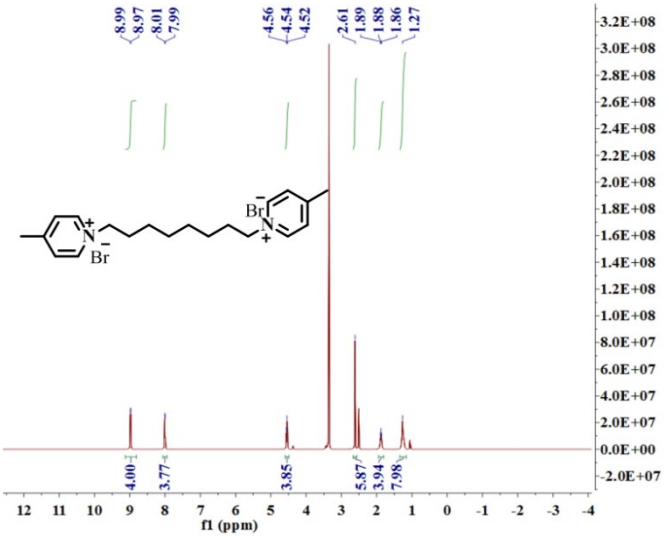

Figure S7 The 400 MHz ^{1}H NMR spectrum of **BDM-3** in the DMSO-d_6 solution.

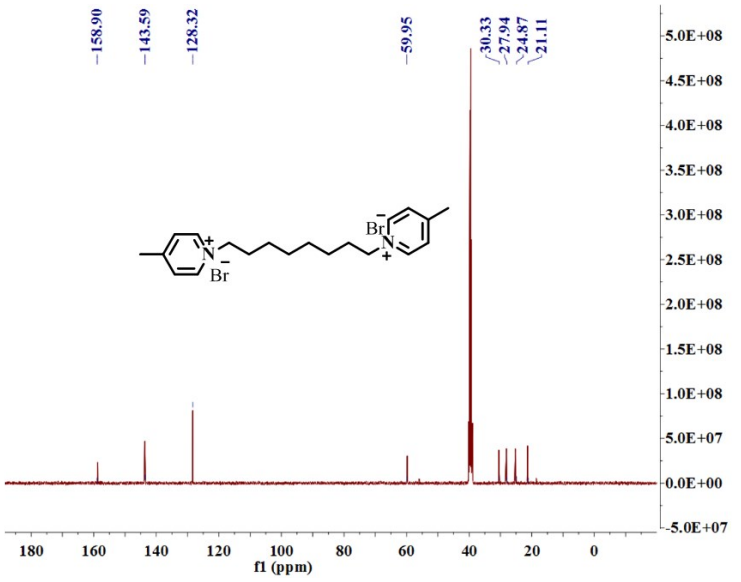

Figure S8 The 100 MHz ^{13}C NMR spectrum of **BDM-3** in the DMSO-d_6 solution.

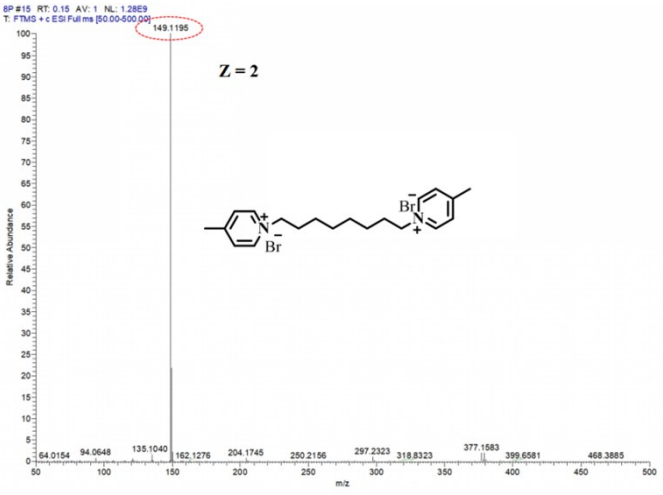

Figure S9 ESI-Mass spectrum of **BDM-3**.

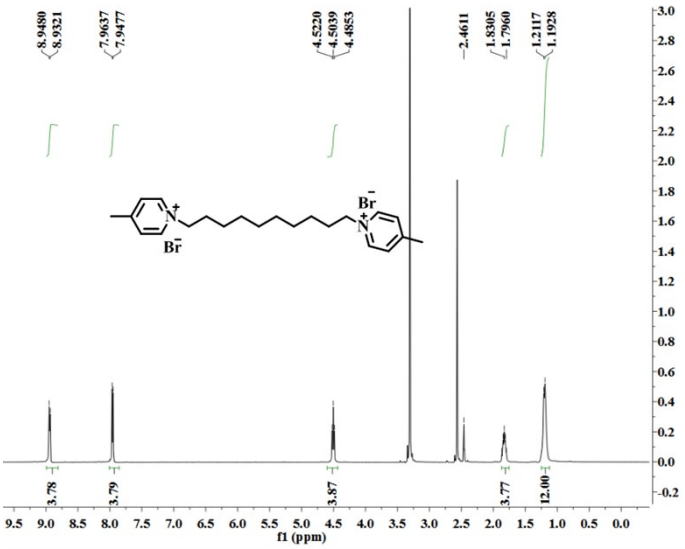

Figure S10 The 400 MHz ^{1}H NMR spectrum of **BDM-4** in the DMSO-d_6 solution.

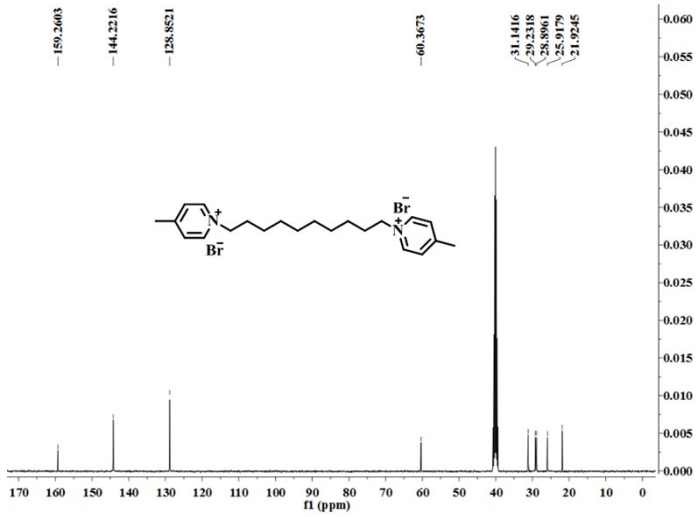

Figure S11 The 100 MHz ^{13}C NMR spectrum of **BDM-4** in the DMSO-d_6 solution.

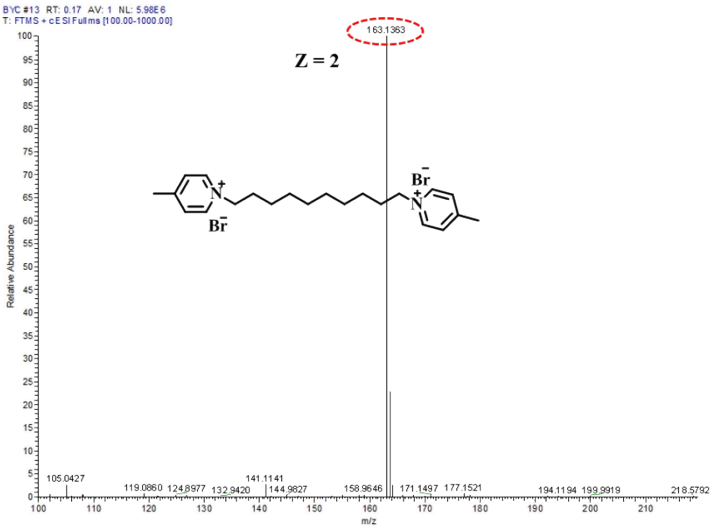

Figure S12 ESI-Mass spectrum of **BDM-4**.

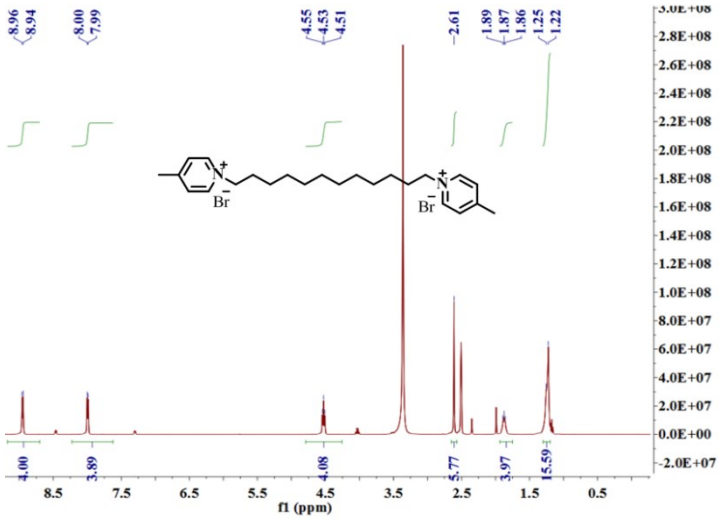

Figure S13 The 400 MHz ^{1}H NMR spectrum of **BDM-5** in the DMSO-d_6 solution.

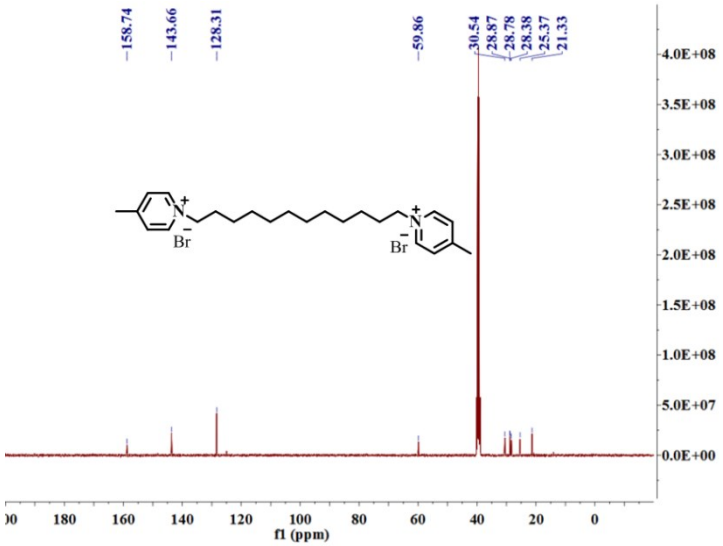

Figure S14 The 100 MHz ^{13}C NMR spectrum of **BDM-5** in the DMSO-d_6 solution.

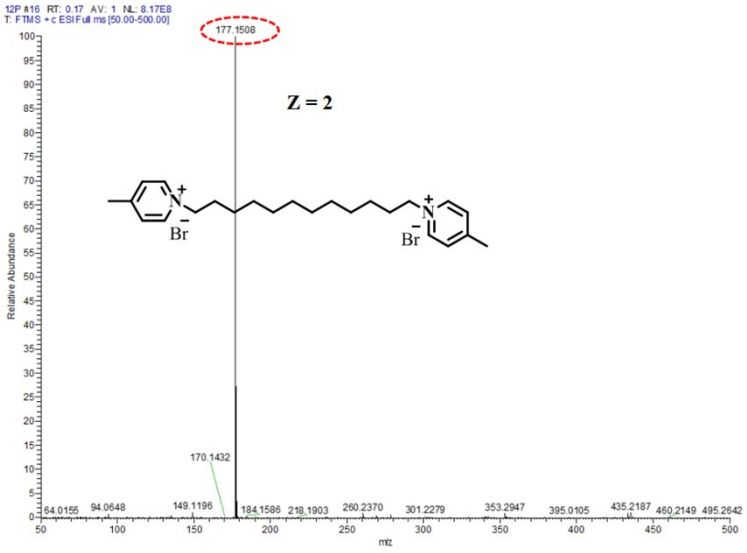

Figure S15 ESI-Mass spectrum of **BDM-5**.

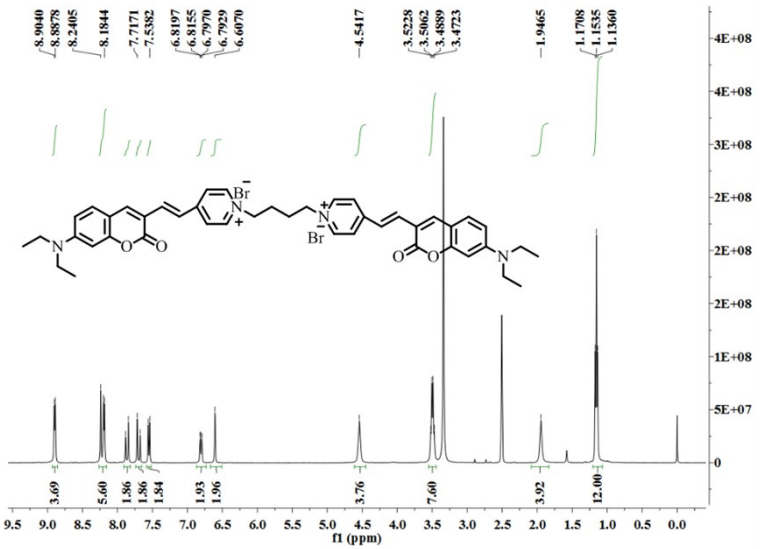

Figure S16 The 400 MHz ^{1}H NMR spectrum of **EBD-1** in the DMSO-d_6 solution.

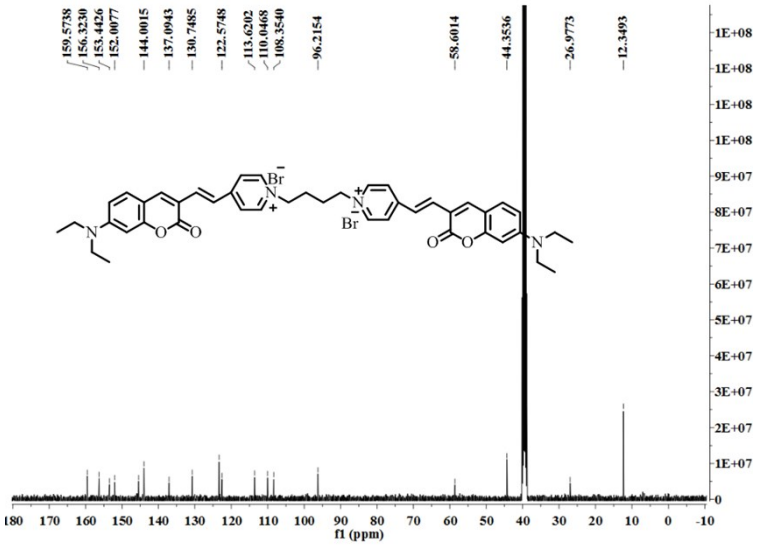

Figure S17 The 100 MHz ^{13}C NMR spectrum of **EBD-1** in the DMSO-d_6 solution.

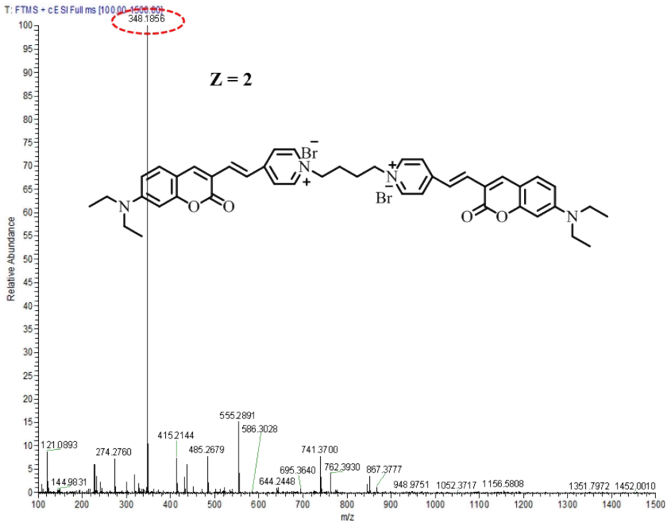

Figure S18 ESI-Mass spectrum of **EBD-1**.

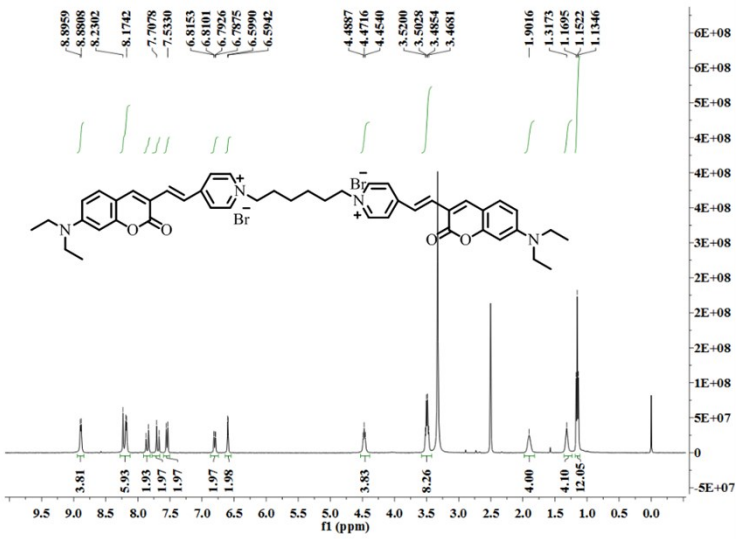

Figure S19 The 400 MHz ^{1}H NMR spectrum of **EBD-2** in the DMSO-d_6 solution.

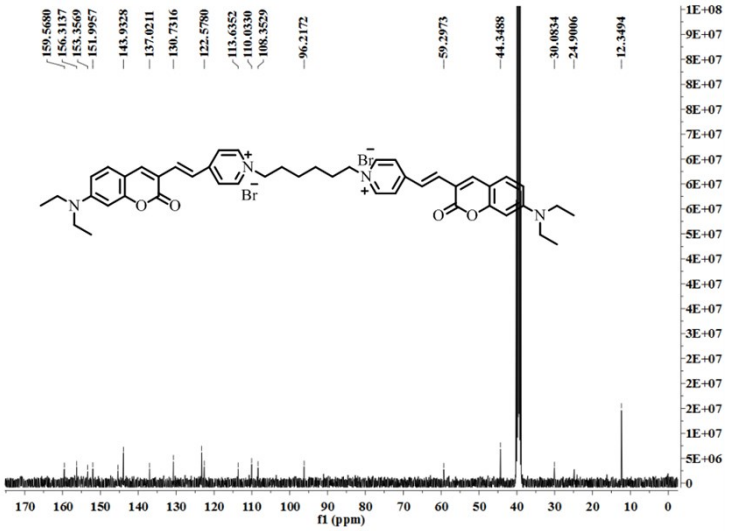

Figure S20 The 100 MHz ^{13}C NMR spectrum of **EBD-2** in the DMSO-d_6 solution.

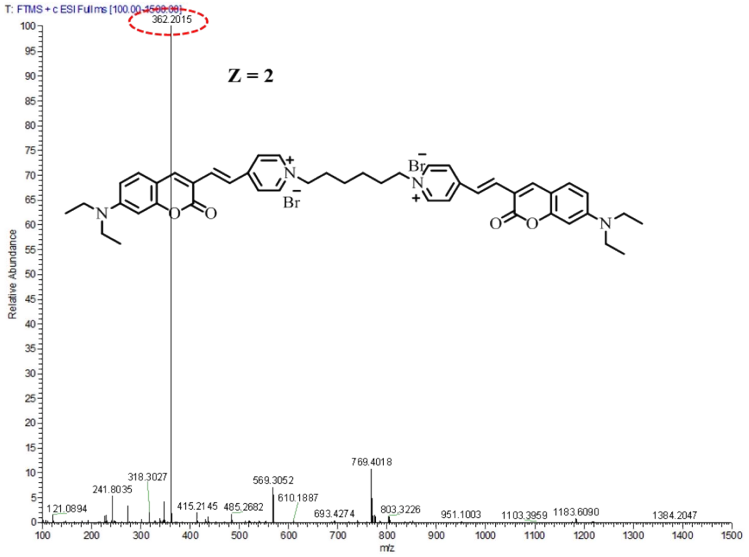

Figure S21 ESI-Mass spectrum of **EBD-2**.

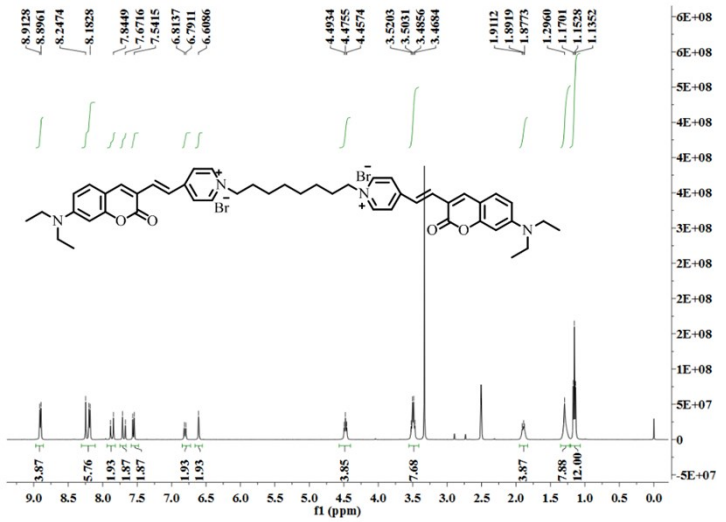

Figure S22 The 400 MHz ^{1}H NMR spectrum of **EBD-3** in the DMSO-d_6 solution.

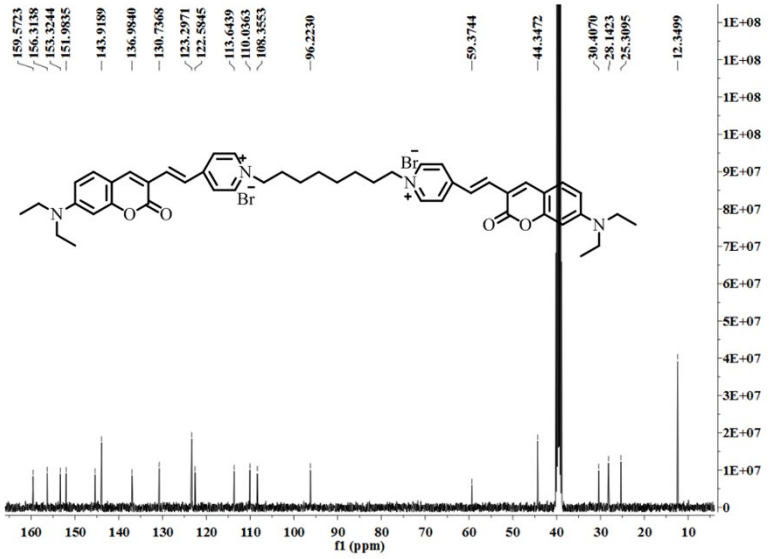

Figure S23 The 100 MHz ^{13}C NMR spectrum of **EBD-3** in the DMSO-d_6 solution.

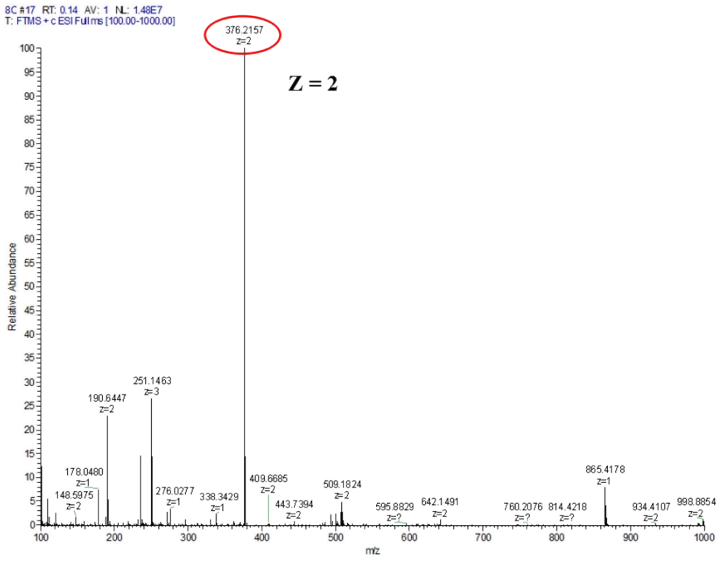

Figure S24 ESI-Mass spectrum of **EBD-3**.

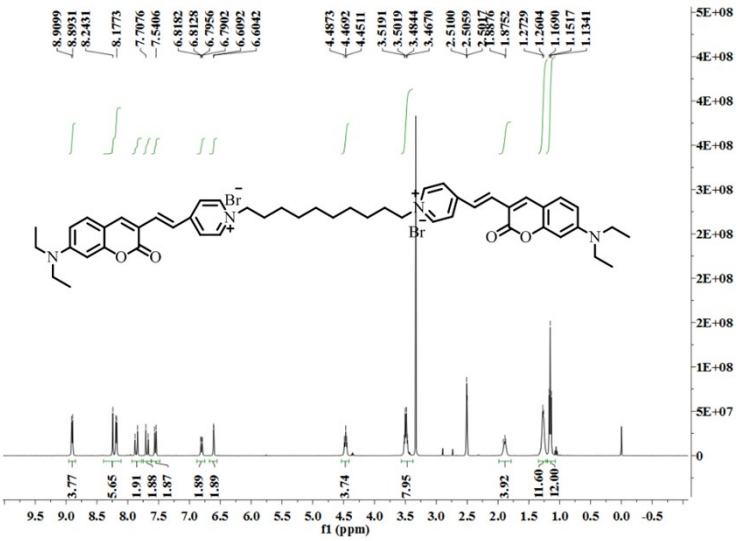

Figure S25 The 400 MHz ^{1}H NMR spectrum of **EBD-4** in the DMSO-d_6 solution.

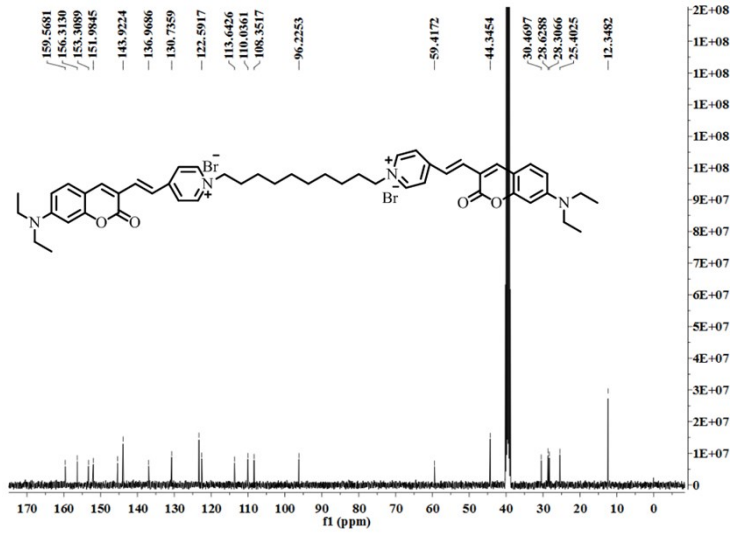

Figure S26 The 100 MHz ^{13}C NMR spectrum of **EBD-4** in the DMSO-d_6 solution.

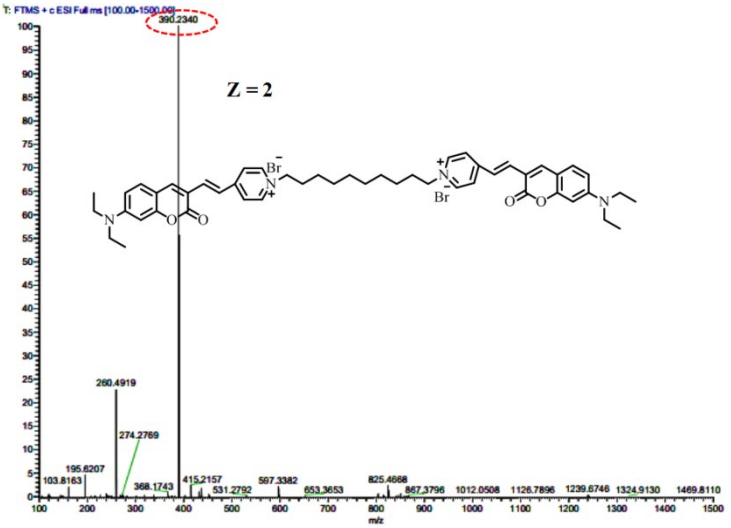

Figure S27 ESI-Mass spectrum of **EBD-4**.

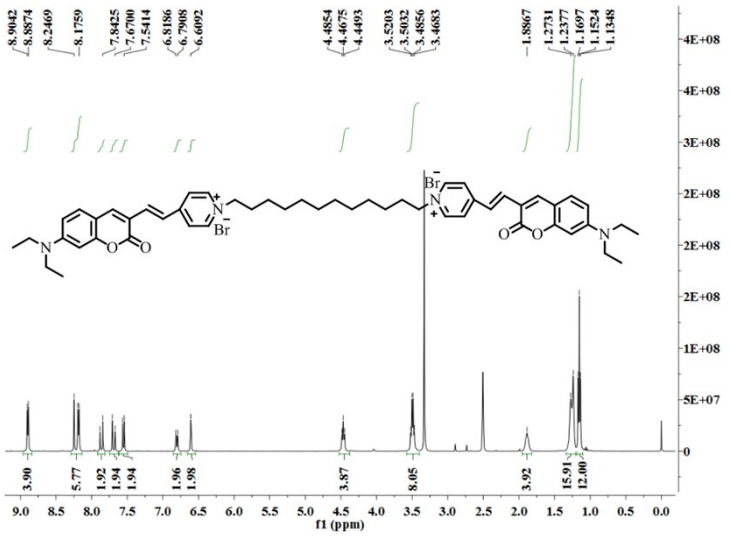

Figure S28 The 400 MHz ^{1}H NMR spectrum of **EBD-5** in the DMSO-d_6 solution.

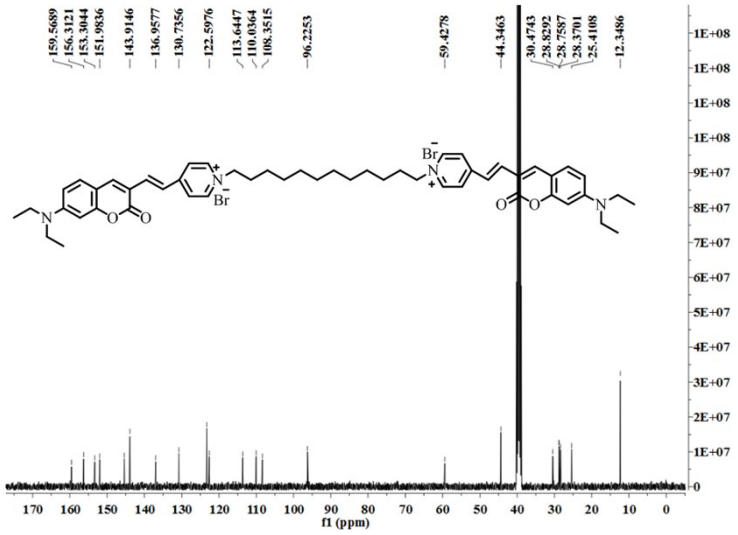

Figure S29 The 100 MHz ^{13}C NMR spectrum of **EBD-5** in the DMSO-d_6 solution.

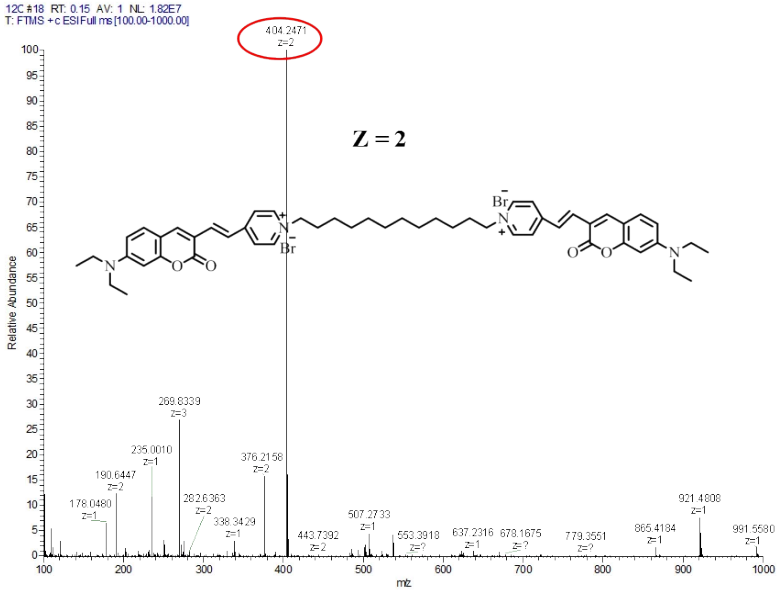

Figure S30 ESI-Mass spectrum of **EBD-5**.

4. Photon-Physical Properties and ROS Generation Ability

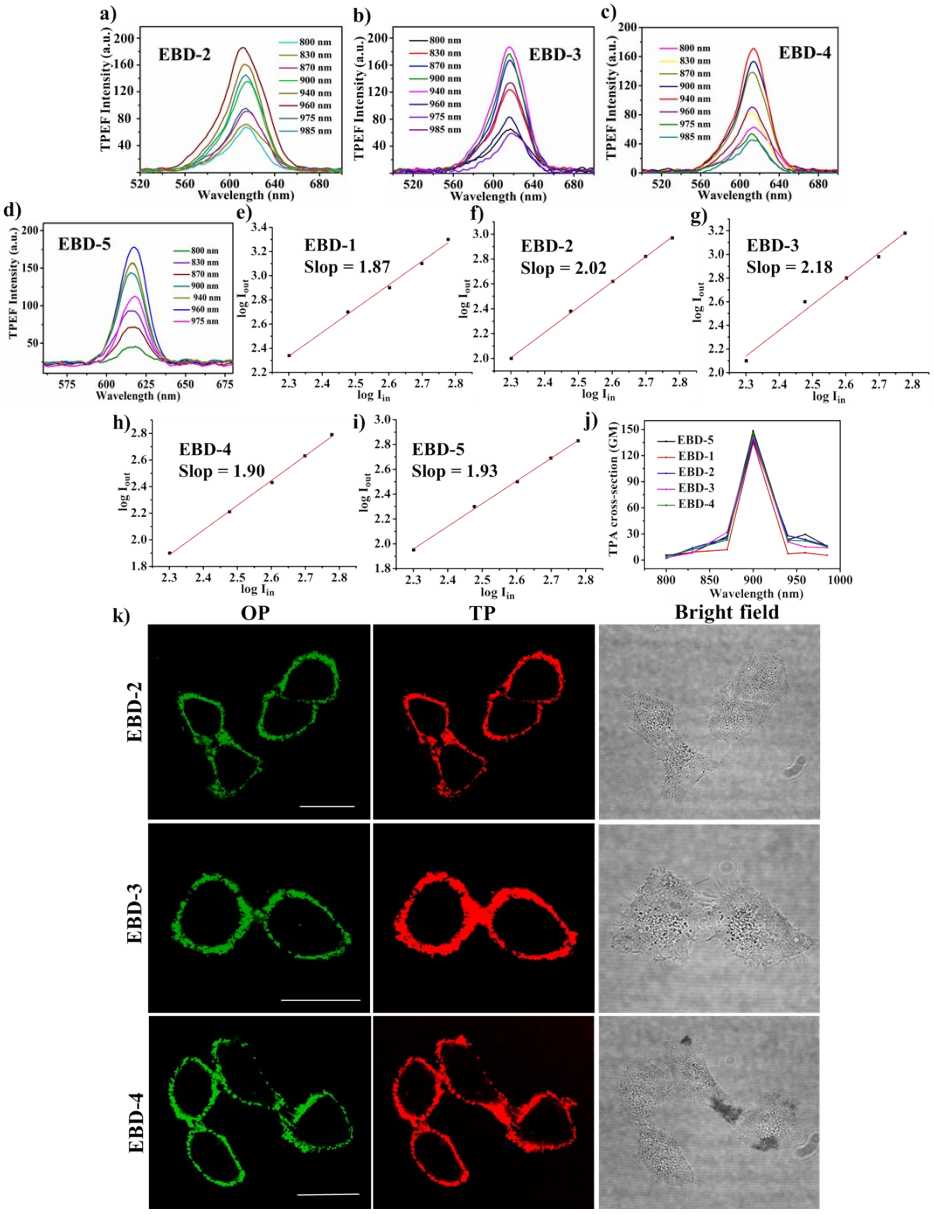

Fig. S31 a-d) Two-photon excited fluorescence spectra of **EBD-2~EBD-5** in 99% glycerin systems. e-i) The verification of two-photon excited fluorescence of **EBD-1~EBD-5** in ethyl alcohol with various laser powers at 960 nm. j) Two-photon absorption cross section of the **EBD-1~EBD-5** (Rhodamine B was used as reference). k) One-photon excitation (OPE) and two-photon excitation (TPE) imaging of HeLa cells pretreated with **EBD-2~EBD-4**. Scale bars: 20 μm.

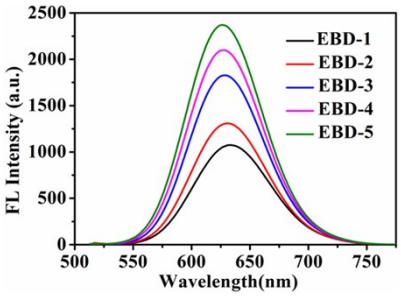

Fig. S32 The fluorescence spectra of **EBD-1**~**EBD-5** in aqueous solution.

Table S1. The photo-physical properties of **EBD-1**~**EBD-5**.

Dyes	λ_{abs} (nm)	ε (x 10^4 M^{-1} cm^{-1})	λ_{em} (nm)	Stock shift (nm)	Φ_{FL} (%)	$\Phi_{^1O_2}$ (%)	ΔE_{st} (ev)
EBD-1	489	7.35	633	144	1.0	90.2	0.71
EBD-2	486	7.69	630	144	9.0	76.5	0.82
EBD-3	485	5.49	628	143	17.0	78.2	0.78
EBD-4	485	8.66	627	142	20.0	82.7	0.81
EBD-5	483	4.46	626	143	26.0	55.5	0.86

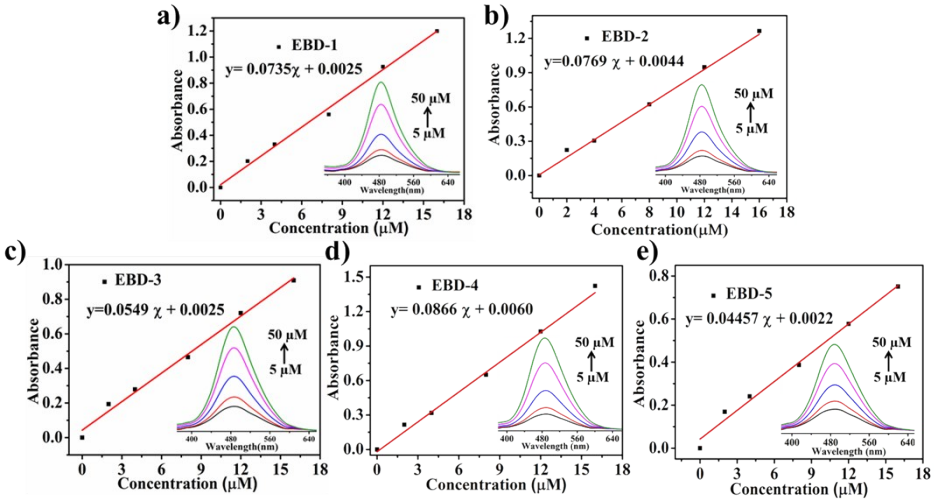

Fig. S33 a) ~e) The molar absorption coefficients (ε) of **EBD-1**~**EBD-5** in aqueous solutions (containing 1% DMSO). Insert: absorption spectra of PSs with different concentrations (5 μM~50 μM).

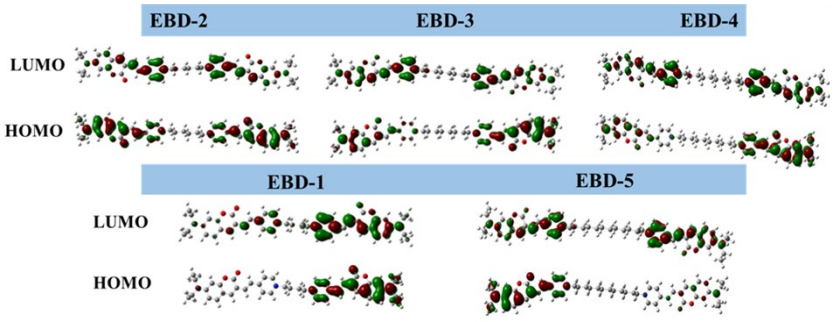

Dyes	EBD-1	EBD-2	EBD-3	EBD-4	EBD-5
ΔE_{st}(eV)	0.71	0.82	0.78	0.81	0.86

Fig. S34 Chemical structures and HOMO-LUMO distributions of **EBD-1~EBD-5**, optimized structures of the HOMO and LUMO at S_1 were calculated by TD-DFT (Gaussian 09/B3LYP/ 6-31G (d)).

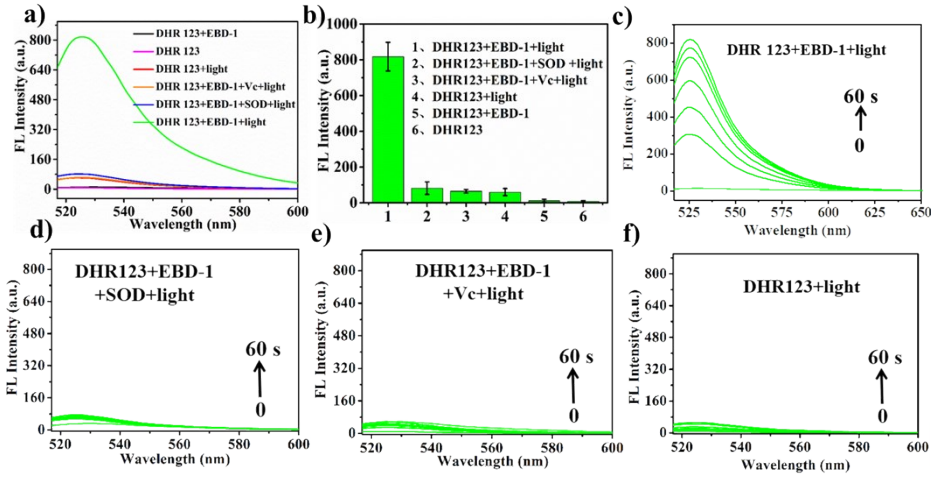

Fig. S35 a) The fluorescence intensity of DHR123 with **EBD-1** under different treatments. b) Quantification of fluorescence intensity of DHR123 in (a) with different treatments. c ~ f) The fluorescence intensity of DHR123 at 528 nm with different treatments under different irradiation time (white light; 20 mW/cm^2 for 60 s).

To further verify the $O_2^{-\bullet}$ production, radical scavenger SOD was further added**.** As expected, the intensity of green fluorescence at 528 nm delivered an 8.0-fold decrease when 10 μM SOD was added into the mixed aqueous solution of DHR123 and **EBD-1**. At the same time, the experiment of **EBD-1** co-added with Vitamin C (Vc), a radical scavenger, was carried out to further see if there is quenching of remaining ROS. As shown in **Fig. S35**, there are not noticeable change in fluorescence signals than co-added with SOD was observed, which didn't look all that different compared to background. Thus, it can be speculated that in our test system (aqueous solution, PS and irradiation condition), there were no more quenching of remaining of ROS.

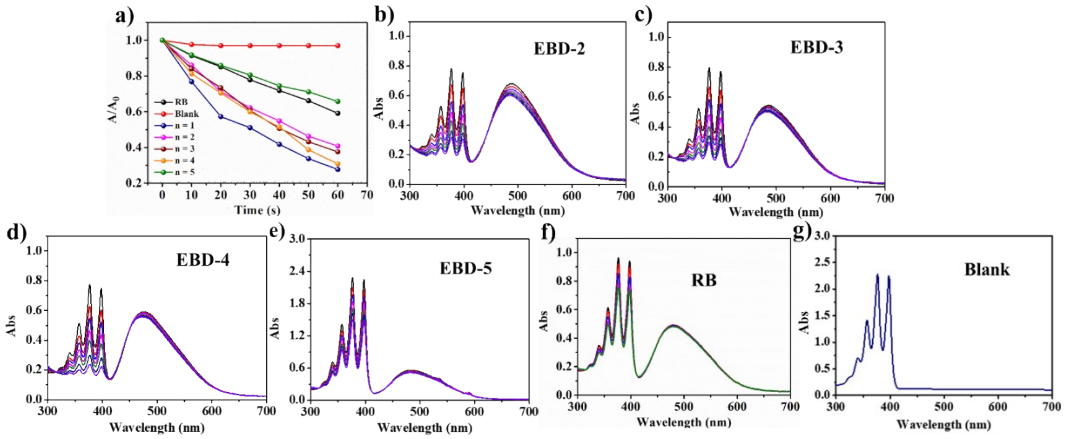

Fig. S36 a) The decomposition rates of ABDA under light irradiation in the presence of different PSs, where A and A_0 represented the absorbance in the presence of ABDA at 378 nm with and without irradiation. b) ~g) The decomposition rates of ABDA in the presence of **EBD-2~EBD-5**, RB and Blank under different irradiation time (white light; 20 mW/cm^2 for 60 s).

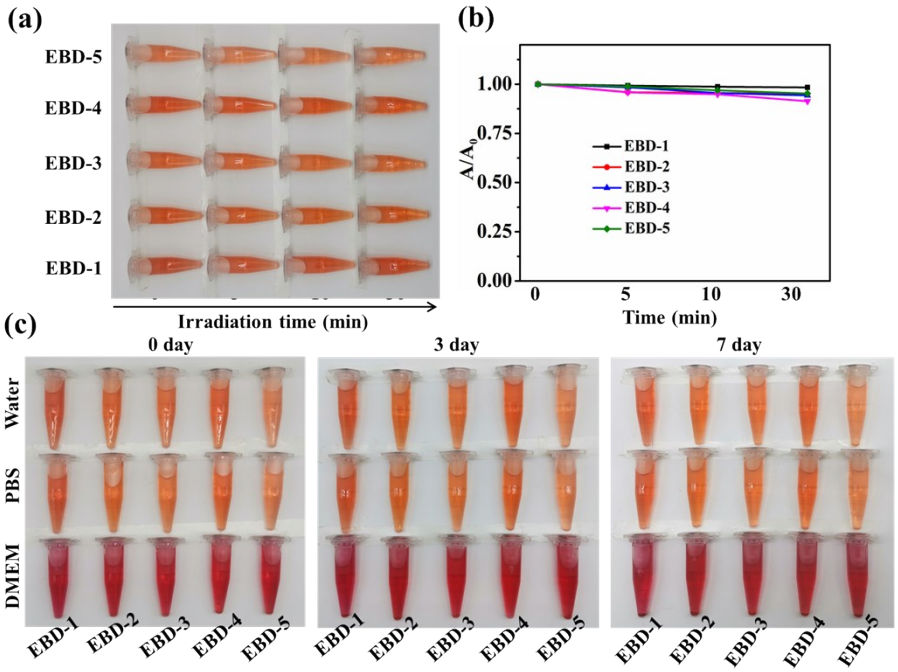

Fig. S37 (a) The stability of **EBD-1~EBD-5** in water, PBS and DMEM media for 0, 3, and 7 days. (b) Photographs of the **EBD-1~EBD-5** in PBS solutions after 808 nm laser (200 mW/cm^2) irradiation for different time. (c) Plot of A/A_0 versus various irradiation time. A and A_0 are the maximal absorption intensity of **EBD-1~EBD-5** in PBS solutions after different irradiation time, respectively.

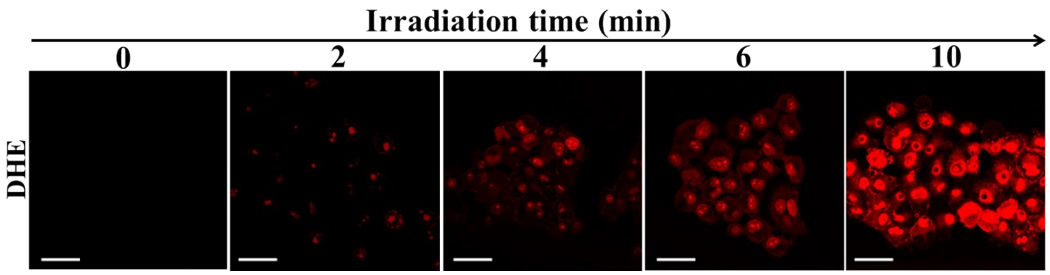

Fig. S38. Fluorescence images of HeLa cells co-stained with **EBD-1**(10 μM) and DHE (λ_{ex} = 488 nm, λ_{em} = 570-620 nm) for 30 min under 808 nm laser irradiation (0, 2, 4, 6, 10 min). Scale bars: 20 μm.

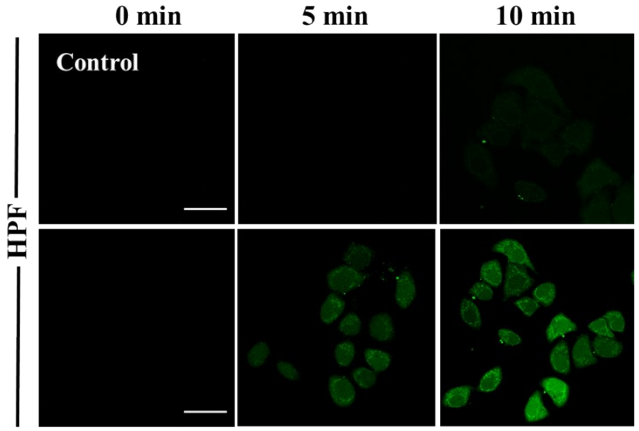

Fig. S39 (a) General OH• in HeLa cells by using HPF (λ_{ex} = 488 nm, λ_{em} = 530 nm) as indicator with different irradiation time (808 nm laser; 200 mW/cm^2). Scale bars: 20 μm.

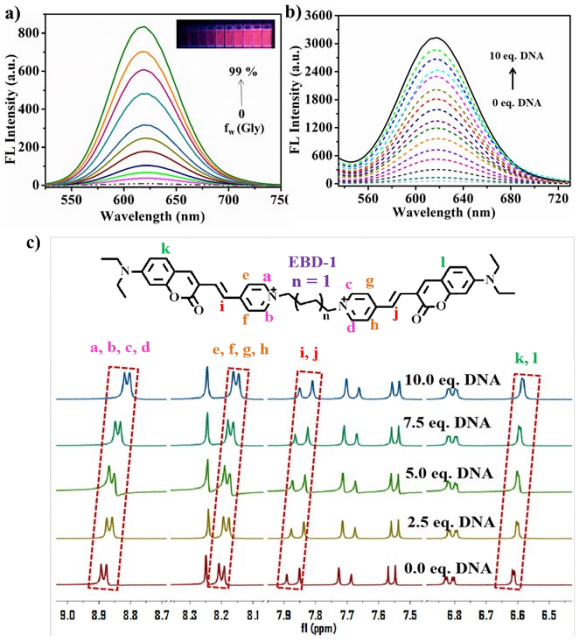

Fig. S40 a) Fluorescence spectra of **EBD-1** under different water and glycerol system (fraction of glycerol: 0~99 %). b) and c) Fluorescence and ^{1}H NMR titration experiments of **EBD-1** (10^{-5} M, DMSO-d_6) with DNA (0-10.0 eq., D_2O-d_2).

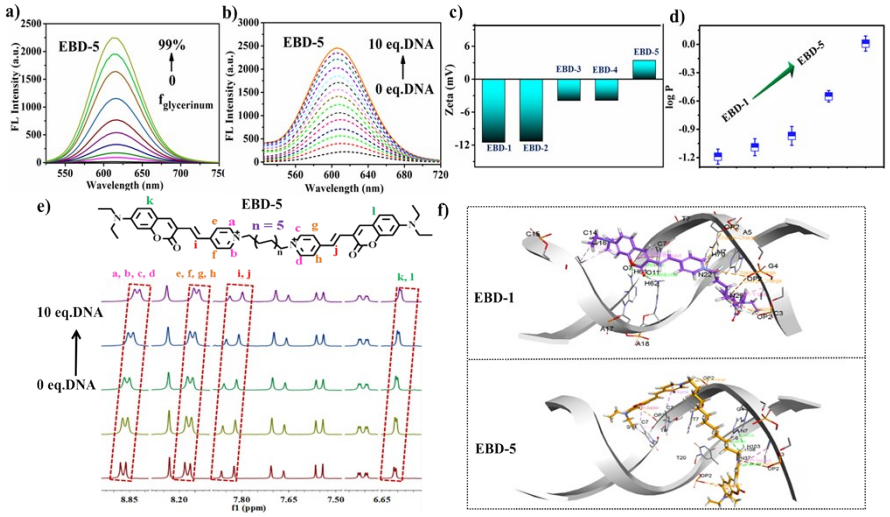

Fig. S41 a) Fluorescence spectra of **EBD-5** under different water and glycerol system (fraction of glycerol: 0~99 %). b) Fluorescence titration of **EBD-5** (10^{-5} M) with DNA (0 – 10.0 eq.). c) Zeta potential of **EBD-1** ~ **EBD-5** in PBS solution (pH = 7.2). d) *N*-octanol-water partition coefficients of **EBD-1** ~ **EBD-5**. e) ^{1}H NMR titration experiments of **EBD-5** (10^{-5} M, DMSO - d_6) with DNA (0 - 10.0 eq., D_2O - d_2). f) Molecular dynamics simulations for the **EBD-1** and **EBD-5** binding with DNA.

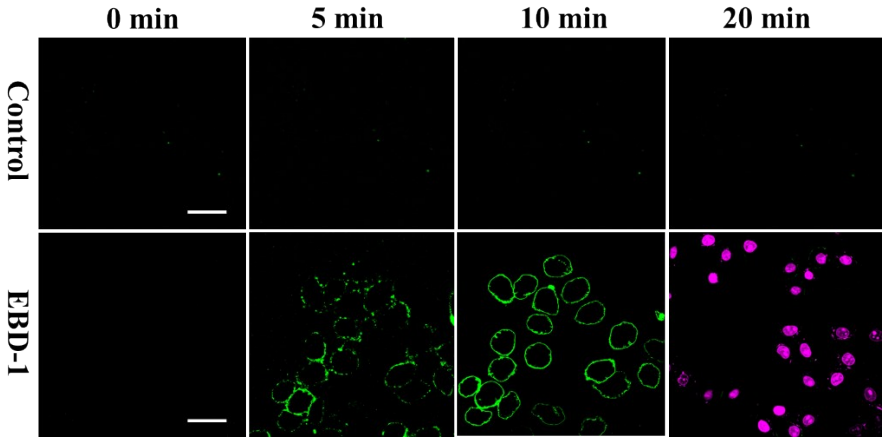

Fig. S42 Merged cell images of apoptosis and necrosis of HeLa cells pre-treated without or with **EBD-1** under NIR laser irradiation at different time intervals. Cells were stained with apoptosis and necrosis assay Annexin V-FITC/PI. Annexin V-FITC (green) (λ_{ex} = 488 nm, λ_{em} = 530 nm), PI (red) (λ_{ex} = 488 nm, λ_{em} = 650-700 nm). Scale bars: 20 μm.

The apoptosis and necrosis assay co-stained with Annexin V-FITC/PI was tested to study cell death mechanism induced by cell membrane-targeting PSs (**EBD-1**). As shown in **Fig. S42**, the control group without light irradiation showed none of fluorescence signal in Annexin V-FITC and PI channel, indicating the normal state without the

occurrence of apoptosis or necrosis. Then, with 808 nm laser irradiation, the as-prepared PSs **(EBD-1**) produced ROS in the plasma membrane to cause major oxidative damage. After 10 min, as shown in the **Fig. S42**, **EBD-1** group exhibited obvious signal on the cell membrane but little fluorescence in the cell nuclei, indicating the occurrence of early stage apoptosis. Moreover, HeLa cells incubated with **EBD-1** under 20 min irradiation showed strong fluorescence signal in cell nuclei and extremely weak signal on the cell membrane, which demonstrated the execution cell necrosis.

Table S2. The binding energy of Ligand **EBD-1** or **EBD-5** with DNA (ID: 1BNA).

Ligand Name	Binding Energy (kcal/mol)	Ligand Energy (kcal/mol)	Protein Energy (kcal/mol)	Complex Energy (kcal/mol)	Entropic Energy (kcal/mol)	Average Binding Energy (kcal/mol)
EBD-1	-436.0719	91.1394	-2507.5255	-2852.458	22.3289	-427.85275
EBD-1	-395.5863	91.874	-2507.5255	-2811.2378	22.3214	
EBD-1	-432.6156	87.4734	-2507.5255	-2852.6678	22.3158	
EBD-1	-452.9145	98.2079	-2507.5255	-2862.2321	22.3164	
EBD-1	-432.231	95.5427	-2507.5255	-2844.2139	22.3272	
EBD-1	-444.7132	94.7874	-2507.5255	-2857.4514	22.3282	
EBD-1	-424.1327	90.1291	-2507.5255	-2841.5291	22.2989	
EBD-1	-421.8606	95.8975	-2507.5255	-2833.4886	22.3242	
EBD-1	-420.4237	94.8904	-2507.5255	-2833.0588	22.3343	
EBD-1	-417.978	94.7842	-2507.5255	-2830.7193	22.3309	
EBD-5	-435.173	42.8133	-2507.5255	-2899.8852	22.7753	-422.44169
EBD-5	-405.7287	43.3442	-2507.5255	-2869.91	22.8223	
EBD-5	-455.6274	38.6724	-2507.5255	-2924.4805	22.8894	
EBD-5	-431.6502	41.4168	-2507.5255	-2897.7588	22.8725	
EBD-5	-422.8633	41.3112	-2507.5255	-2889.0776	22.8426	
EBD-5	-392.2164	40.9691	-2507.5255	-2858.7728	22.8445	
EBD-5	-428.0516	37.6567	-2507.5255	-2897.9205	22.8294	
EBD-5	-455.7948	45.5045	-2507.5255	-2917.8158	22.8657	
EBD-5	-420.4727	43.2962	-2507.5255	-2884.7019	22.8559	
EBD-5	-376.8388	40.1483	-2507.5255	-2844.216	22.7851	

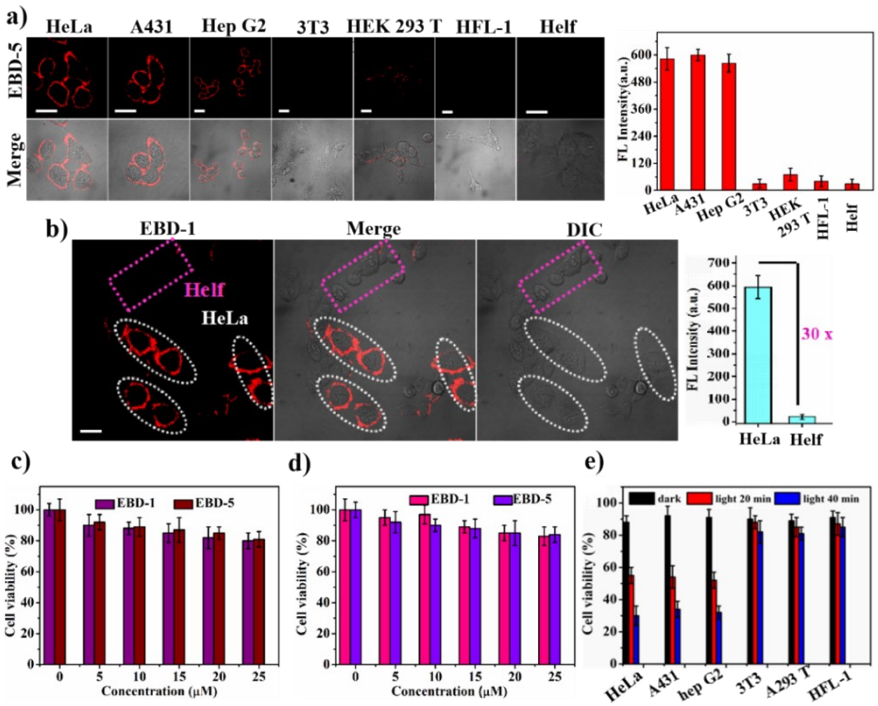

Fig. S43 a) Confocal images of three cancer cells (HeLa, A431, Hep G2) and four normal cells (3T3, HEK 293T, HFL-1 and Helf), which incubated with **EBD-5** (10^{-5} M) for 30 min. Right: fluorescence intensity of different cell lines stained by **EBD-5**. b) Fluorescence intensity distribution of HeLa (white circle) and Helf cells (purple circle) cultivated in the same dish. Right: fluorescence intensity of the two cell lines stained by **EBD-5**. c) Cell viability of **EBD-1** and **EBD-5** treated with HeLa cells with different concentrations (0~25 μM). d) Cell viability of **EBD-1** and **EBD-5** treated with Helf cells with different concentrations (0~25 μM). e) Cell viability of **EBD-5** treated with different cells with different treatment (**EBD-5**, 10 μM). All of fluorescence intensity of different cell lines obtained by the cell image processing software Image J. Scale bar = 20 μm.

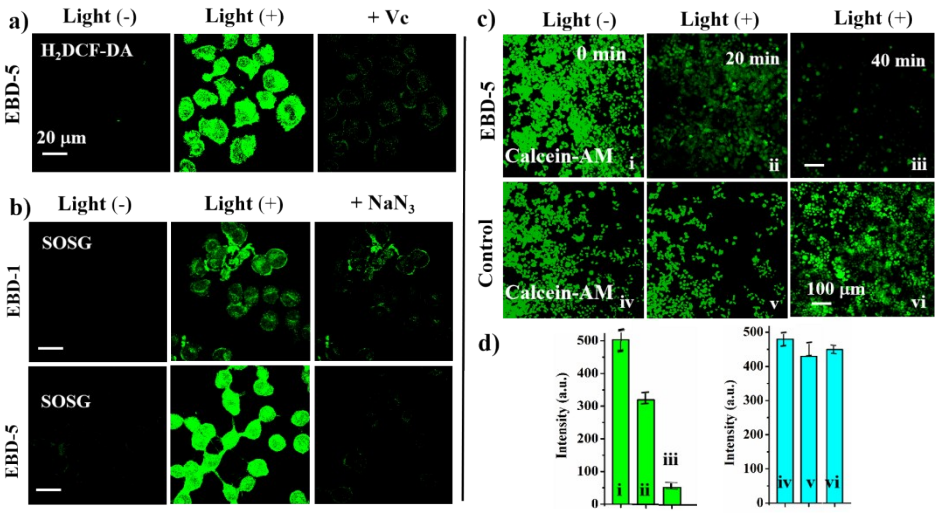

Fig. S44 a) Intracellular ROS imaging in the absence or presence of Vc and **EBD-5** using H_2DCF-DA (λ_{ex} = 504 nm, λ_{em} = 529 nm) as indicator. b) Intracellular $^1O_2$ generation of **EBD-1** and **EBD-5** using SOSG (λ_{ex} = 504 nm, λ_{em} = 525 nm) as indicator among NaN_3 was obtained to clear free radical. c) Live assays of HeLa cells treated as follows: group 1: Calcein AM + **EBD-5** + irradiation for 0 min, 20 min or 40 min, group 2: Calcein AM +irradiation for 0 min, 20 min or 40 min). Green channel for Calcein AM (λ_{ex} = 490 nm, λ_{em} = 515 nm). d) Green fluorescence intensity acquired by Image J software, which indicated the HeLa cells activity. Left: Experiment group; Right: Control group.

For evaluating intracellular ROS generation ability of **EBD-5**, a commercial probe, non-emission 2, 7-dichloro fluorescein diacetate (H_2DCF-DA) that emitted green fluorescence immediately when reacting with ROS, which was used to detect intracellular ROS under irradiation. As presented in **Fig. S44a**, HeLa cells were co-cultured with H_2DCF-DA and **EBD-5** without or with light illumination for 30 min, which showed obvious green fluorescence enhancement at a short time, suggesting much ROS generation during PDT process, which was also supported by ROS scavenging assay (50 μM Vc was added)

Then SOSG was used for ROS scavenging specific ROS generation ($^1O_2$), which showed green fluorescence in treated HeLa cells after 10 min light irradiation (HeLa cells were co-cultured with SOSG and **EBD-n**). Moreover, the $^1O_2$ induced by **EBD-1** or **EBD-5** was completely scavenged by NaN_3 (a widely accepted $^1O_2$ scavenger), further implying the produced ROS was $^1O_2$ (**Fig. S44b**).

To intuitively evaluate the kill capability of **EBD-5** to cancer cells during light-triggered PDT process, standard living cell commercial dye Calcine AM showing green fluorescence was obtained to monitor cell activity. As depicted in **Fig. S44c**, group 1: Calcein AM + **EBD-5** + irradiation for 0 min, 20 min or 40 min, group 2: Calcein AM + irradiation for 0 min, 20 min or 40 min were respectively performed to detect invisible apoptosis signals. As

expected, both group 1 and group 2 exhibited strong green fluorescence in whole cytoplasm before irradiation, indicating high cellular activities could still be observed. But, decreased green fluorescence were observed in experimental group (group 1) under 20 min irradiation while no obvious fluorescence change was observed in control group (group 1), which were also in line with the fluorescence intensity (**Fig. S44d**). All the above represented that **EBD-5** mediated PDT could generate a certain amount of high-toxic ROS to kill cancer cells during photon-triggered PDT process.

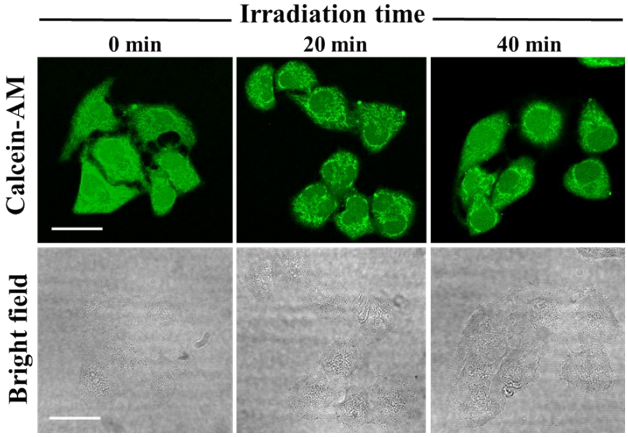

Fig. S45 HeLa cells treated with Calcein AM and **EBD-1** with irradiation for different time (0, 20, 40 min). Scale bar = 20 μm.

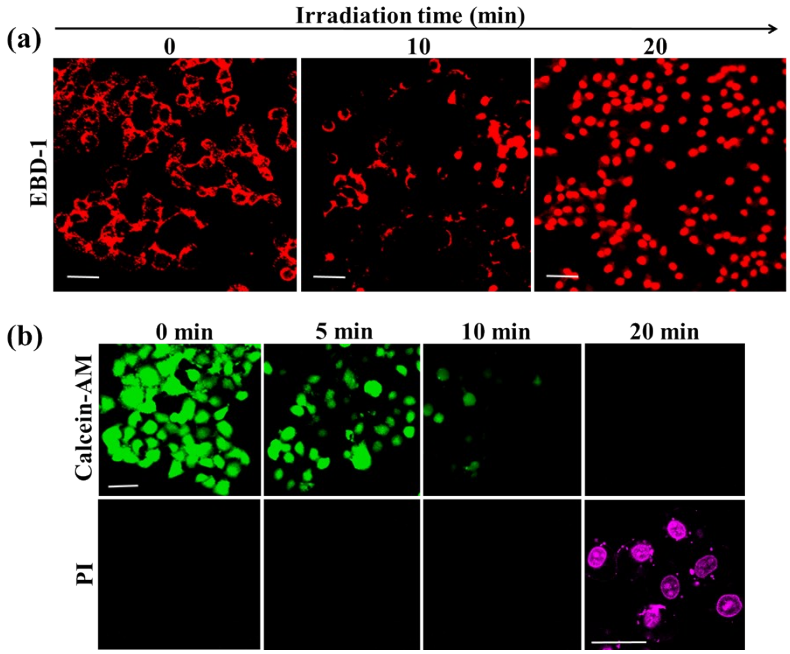

Fig. S46 (a) Confocal fluorescence imaging of HeLa cells pretreated with **EBD-1 (**10 uM**)** under different irradiation time (808 nm laser; 200 mW/cm^2). (b) Commercial live/dead stain assay (Calcein-AM/PI) (Calcein-AM: λ_{ex} = 490 nm; λ_{ex} = 515 nm, PI: λ_{ex} = 488 nm; λ_{ex} = 650-700 nm) were co-cultured with **EBD-1** to monitor the cell viability.

Scale bar = 20 μm

As shown in **Fig. S46a,** confocal fluorescence imaging of HeLa cells pretreated with **EBD-1** indicated that, with irradiation, our as-prepared PSs gradually transferred from plasma membrane to nucleus, indicating the decreased cell viability. After a total irradiation of 20 min, the fluorescence signal can only be found in cell nuclei, which suggested the cell death.

To intuitively evaluate the killing effect on HeLa cells, the standard live/dead stain assay (Calcein-AM/PI) were used to monitor the state of cell life. As depicted in **Fig. S46b**, only strong green fluorescence in whole cytoplasm was visualized by CLSM before irradiation, indicating high activity of cancer cells. However, continuous irradiation for 20 min, the disappeared green fluorescence and the increased bright fluorescence signal in all nucleus area suggested that all HeLa cells lost cell viability, which was in line with the result of **Fig. S46a**, indicating **EBD-1** can self-report the cell viability.

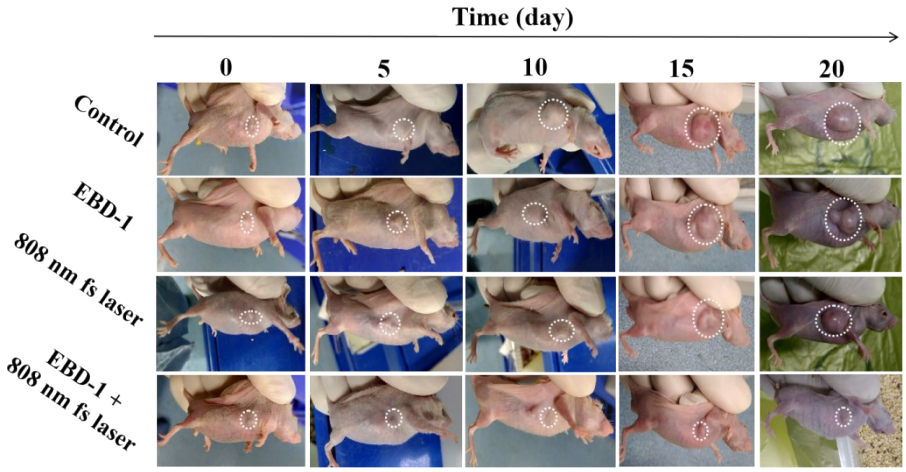

Fig. S47 a) Photographs of A431 tumor-bearing mice of four groups taken during 20 d period after various treatments.

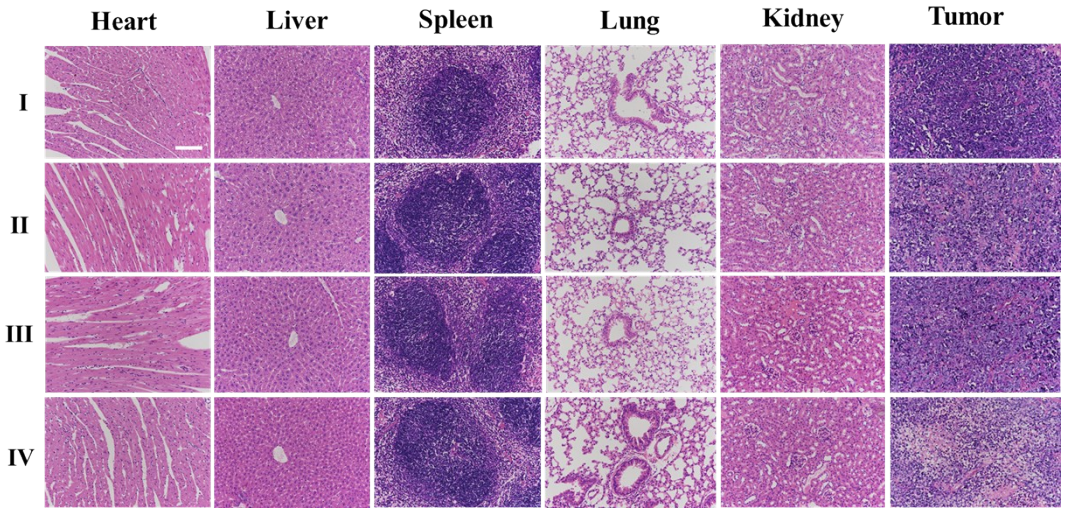

Fig. S48 Hematoxylin and eosin (H&E)-stained major organs and tumor after therapy with **EBD-1**. Scale bars: 100 μm.

Notes and References

[S1] H. Xu, H. Zhang, G. Liu, L. Kong, X. Zhu, X. Tian, Z. Zhang, R. Zhang, Z. Wu, Y. Tian and H. Zhou, Anal. Chem., 2019, 91, 977-982.

[S2] H. R. Drew, R. M. Wing, T. Takano, C. Broka, S. Tanaka, K. Itakura and R. E. Dickerson, PNAS., 1981, **78**, 2179-83.

[S3] K. Wang, Y. Lei, J. Chen, Z. Ge, W. Liu, Q. Zhang, S. Chen, Z. Hu, *Dyes and Pigments*., 2018, **151**, 233-237.